

9427 8213 NACA TN 3129 7246

0065978



TECH LIBRARY KAFB, NM

NATIONAL ADVISORY COMMITTEE FOR AERONAUTICS

TECHNICAL NOTE 3129

INVESTIGATION OF A SLAT IN SEVERAL DIFFERENT POSITIONS
ON AN NACA 64A010 AIRFOIL FOR A WIDE RANGE OF
SUBSONIC MACH NUMBERS

By John A. Axelson and George L. Stevens

Ames Aeronautical Laboratory
Moffett Field, Calif.



Washington
March 1954

AFMTC

TECHNICAL LIBRARY

AFL 2611



0065978

NATIONAL ADVISORY COMMITTEE FOR AERONAUTICS

TECHNICAL NOTE 3129

INVESTIGATION OF A SLAT IN SEVERAL DIFFERENT POSITIONS

ON AN NACA 64A010 AIRFOIL FOR A WIDE RANGE OF

SUBSONIC MACH NUMBERS

By John A. Axelson and George L. Stevens

SUMMARY

An investigation of the two-dimensional aerodynamic characteristics of an NACA 64A010 airfoil with a slat has been conducted in the Mach number range from 0.25 to 0.85, with a corresponding Reynolds number range from 3.4 million to 8.1 million. Two families of slat positions were investigated, one with the slat leading edge extended forward along the airfoil chord line, and the other with the slat extended forward and displaced below the chord line.

The results indicate that for section lift coefficients up to 0.6, the airfoil with the slat retracted generally was aerodynamically superior to any of the other airfoil-slat arrangements investigated. The drags with the slat nose on the extended chord line were only slightly higher than the drag with slat retracted, whereas displacing the slat nose below the chord line markedly decreased the drag-divergence Mach number. Above 0.7 section lift coefficient and at the higher test Mach numbers, the best results were obtained with the slat nose on the extended chord line of the airfoil.

At the lower test Mach numbers, the highest maximum lifts were measured with the slat nose displaced below the wing chord line. At supercritical speeds, however, adverse effects such as occur with cambered airfoils resulted with the slat nose below the airfoil chord line. These adverse effects were large increases in drag and in angle of attack for zero lift and large negative trim changes.

INTRODUCTION

High-lift devices have been used extensively for improving the landing and take-off performance of all types of airplanes. One of these devices, the leading-edge slat, has been used to increase maximum lift and lift-drag ratio and, also, to improve lateral stability and control at high angles of attack by delaying the stall over the outer portions of the

wing and ailerons. In recent years the use of slats and wing leading-edge modifications has been directed at improving the characteristics of swept wings at high speeds as well as at low speeds. Further research also appears desirable on the development of slats for use on thin unswept wings suitable for supersonic flight.

The low-speed investigation reported in reference 1 indicated that the then generally accepted rules for slat design were not applicable to thinner wings suitable for high-speed use. Further, the optimum slat location varied widely with slat size and generally involved a compromise between as large a maximum lift as possible and a minimum change in lift at the prestall incidence for opening of the slat. Additional two-dimensional investigations of slats and leading-edge flaps are reported in references 2 and 3. Although higher maximum lifts have generally been obtained with slats than with the other leading-edge devices, insufficient information is available concerning their relative merits, especially at higher speeds. The present investigation was undertaken to provide information on the behavior of slats on a two-dimensional airfoil over a wide range of subsonic Mach numbers.

NOTATION

c	airfoil chord length with slat retracted, ft
c_d	section drag coefficient, $\frac{\text{drag}}{qS}$
c_l	section lift coefficient, $\frac{\text{lift}}{qS}$
c_m	section pitching-moment coefficient referred to quarter-chord axis, $\frac{\text{pitching moment}}{qSc}$
c_{m_0}	section pitching-moment coefficient at zero lift
M	free-stream Mach number
P	pressure coefficient, $\frac{\text{local static pressure} - \text{free-stream static pressure}}{q}$
ΔP	incremental pressure coefficient, difference between pressure coefficients for upper and lower surfaces
P_{cr}	critical pressure coefficient, corresponding to local sonic velocity

q	free-stream dynamic pressure, lb/sq ft
S	area of airfoil with slat retracted, sq ft
X	forward displacement of slat leading edge, ft
x	chordwise coordinate of airfoil section, percent chord
Y	downward displacement of slat leading edge below airfoil chord line, ft
y	local half-thickness ordinate of airfoil section, percent chord
α_0	section angle of attack of airfoil chord line, deg
δ	angle between slat center line and airfoil chord line, deg

APPARATUS AND TESTS

Wind Tunnel and Model

The channel used for two-dimensional testing of airfoils and slats in the Ames 16-foot high-speed wind tunnel is shown in figure 1. The installation consisted essentially of two walls, each having a thickness of 6 inches and being mounted vertically to form an 18-inch-wide, two-dimensional channel, 16 feet high. The airfoil used in the present investigation had the NACA 64A010 section. The coordinates and details of the airfoil and slat are shown in figure 2. The parting lines between the main airfoil and the slat occurred at 4.7-percent chord on the lower surface and at 17.0-percent chord on the upper surface of the combination. The model was mounted on the strain-gage balance shown schematically in figure 3.

The spaces between the ends of the model and the walls were sealed by sheets of cork faced with felt and held firmly against the walls by inflatable neoprene bladders (fig. 3). The air pressure in these bladders was regulated so as to introduce no measurable interference on the force readings. The airfoil model had a span of 18 inches and a chord of 24 inches. The slat and airfoil were provided with one chordwise row of static-pressure orifices connected to a mercury-filled manometer which was photographed to obtain the pressure records.

Precision

The estimated accuracies of the various aerodynamic results presented in the figures are as follows:

	<u>M = 0.25 to 0.40</u>	<u>M = 0.50 to 0.85</u>
c_l	± 0.01	± 0.007
c_d	± 0.005	± 0.003
c_m	± 0.005	± 0.003
α_0	$\pm 1^\circ$	$\pm 1^\circ$
M	± 0.01	± 0.01
P	± 0.02	± 0.02

Tests

The Mach number range of this investigation was from 0.25 to 0.85 with a corresponding Reynolds number range from 3.4 million to 8.1 million. The variation of average Reynolds number with Mach number is shown in figure 4. The angle-of-attack range was from -4° to 20° at the lower test Mach numbers but was limited by model strength at the higher Mach numbers.

No corrections have been applied to the results since it was found that for the small ratio of model chord to tunnel height (0.125), the tunnel-wall and blockage corrections to the force coefficients and Mach number calibration were extremely small.

All section force coefficients presented in this report were computed from the balance measurements. Section normal-force coefficients computed from integrations of the pressure distributions were in close agreement with those from the balance measurements.

RESULTS AND DISCUSSION

Presentation of Results

All section force coefficients are presented in tables I through VII. Representative lift, drag, and pitching-moment results for a low and a high subsonic Mach number are presented in figures 5, 6, and 7, respectively. Because of model-strength limitations, maximum lifts were obtained at the lower speeds only. In most cases, however, results were obtained up to section lift coefficients where the drag-rise rates with increasing lift and with increasing Mach number were fairly high. The drag results are summarized in figure 8. The section pitching-moment

coefficients at zero lift are summarized in figure 9. Chordwise pressure and load distributions are presented in figures 10 and 11 for the airfoil with the slat retracted and in positions D and F.

Lift

Maximum lift was obtained for all seven airfoil-slat arrangements only at a Mach number of 0.40. The lift curves for Mach numbers of 0.40 and 0.82 are presented in figure 5. The highest section lift coefficients at low Mach numbers were obtained with the slat in position F, displaced below the chord line. The increment in maximum section lift coefficient produced by the slat at 0.40 Mach number was about 0.5. A greater increase in maximum section lift coefficient was obtained in the investigation reported in reference 2 with a similar model but with increased downward displacement and deflection angle of the slat.

Displacing the slat nose below the airfoil chord line (positions E, F, and G, fig. 2) resulted in the addition of positive camber to the resulting airfoil-slat combination, while the resulting chord line through the slat nose was rotated $3^{\circ}9'$ below the reference chord line of the basic airfoil. The net effect was an increase in the angle of attack for zero lift for the drooped slat arrangements, which, for example, amounted to 2° at 0.40 Mach number with the slat in position F. The adverse effects of camber at supercritical speeds increased the zero lift angles, which, for slat position F, increased to 5° at 0.82 Mach number. Information on the effects of camber on zero-lift angle and on stability and control at high subsonic speeds may be found in reference 4.

For slat positions B, C, and D, the reference chord line of the basic airfoil passed through the nose of the airfoil-slat combination. However, the different angle settings of the slat resulted in small camber effects as indicated in figure 5, where the angles of attack for zero lift at 0.40 Mach number varied from $1-1/2^{\circ}$ for position B to $1/2^{\circ}$ for position D. These zero lift angles remained essentially constant over the test range of Mach numbers. For independently operating slats, position D appears to be the best of those investigated because it offers the possibility of increasing the maximum section lift coefficients while providing a minimum change in lift at the angle of attack for opening of the slat, which, in this case, should be around 7° at 0.40 Mach number.

These results should not be interpreted as ruling out the incorporation of a limited amount of droop in a slat for use at higher speeds. With regard to swept wings, extension of slats may improve the aerodynamics of the wing as a result of changes in the plan form and in the vorticity shed from the wing as well as from the changes in airfoil section characteristics. These other effects must be considered when

designing slats for use at high subsonic speeds on swept wings, but, as yet, experimental investigation and existing results provide the only means for evaluating their magnitudes.

The somewhat lower values of maximum section lift coefficient obtained for the basic airfoil with the slat retracted (position A) as compared to those values shown in reference 5 for the same section may be attributed to the discontinuity in profile which existed at the trailing edge of the retracted slat. Agreement exists with those results in reference 5 for the airfoil with roughness added to the surface.

Drag

The drag polars in figure 6 and the summary curves in figure 8 indicate that for section lift coefficients up to about 0.6, the best drag characteristics were obtained with the slat retracted. The increases in angle of attack for zero lift with increasing Mach number which were noted for the drooped slat positions E, F, and G were accompanied by large increases in section drags, as indicated in figures 8(a) and 8(b).

The profile discontinuity at the trailing edge of the retracted slat and possibly the effects of side-wall interference resulted in larger values for the minimum section drag coefficient for the basic airfoil of the present investigation as compared to that shown in reference 5.

For section lift coefficients of 0.8 and 1.0 (figs. 8(d) and 8(e)), superior drag characteristics were generally obtained with the slat in positions D, E, and F, where large increases in the Mach number for drag divergence were obtained. At 0.40 Mach number and above a section lift coefficient of 1.1, the drag was least with the slat in position F. The results for slat position E are especially interesting. As shown in figure 6, the smallest drags and the best lift-drag ratios at 0.40 Mach number between section lift coefficients of 0.7 and 1.1 were obtained with position E, which involved a closed gap and, consequently, no flow of air through the gap. In reference 6, emphasis is placed on the importance of the energizing effect attributed to the air flowing through the gap and acting to accelerate the boundary layer on the upper surface of the airfoil. The results of the present investigation are not explainable by this approach, but suggest that a better concept of slat performance might be gained from a consideration of the camber and loading effects produced by the slat. This will be discussed further in the section on pressure distribution.

Above 0.70 Mach number the best drag results at high section lift coefficients were obtained with the slat on the extended airfoil chord line in positions C and D. The latter position, however, appeared the more promising of these two because of its better characteristics at Mach numbers below 0.70

Pitching Moment

Extending the slats caused a forward movement of the aerodynamic center at all speeds. In the vicinity of maximum lift, the pitching moments decreased abruptly with increasing angle of attack. The forward shift in aerodynamic center can be attributed largely to the 9-percent increase in chord and area produced by the forwardly extended slat. The results shown in figure 9 indicate that drooping the slat produced a negative section pitching moment at zero section lift similar to the negative force couple which exists on a cambered airfoil near zero lift. The magnitude of the negative section pitching-moment coefficient increased at the higher Mach numbers, reflecting the changes in loading over the drooped slats and the forward portion of the airfoil.

Pressure Distribution

Pressure distributions for several angles of attack and for Mach numbers of 0.50, 0.70, and 0.80 are presented in figure 10 for the airfoil with the slat retracted, in position A, and in positions D and F, which were considered to be the most promising of each of the two types of slat positions investigated. The pressure distributions indicate that extending the slats with the airfoil at high angles of attack eliminated separation, as evidenced by the greater pressure recovery on the upper surface near the trailing edge of the airfoil, and increased the pressure on the lower surface of the airfoil. The chordwise distributions of loading shown in figure 11 illustrate more clearly than does figure 10 the gain in lift over the slat and the forward portion of the airfoil at high angles of attack.

The adverse effects of the drooped slats at the lower angles of attack are evidenced in both figures 10 and 11 by the reversed or downward loads which occurred on the slat in position F. The air flow broke away from the abrupt profile discontinuity on the lower side of the slat and remained detached over the forward half of the lower surface of the airfoil. This detached flow appears to have been the primary cause of the large drag at low section lifts noted for the drooped slat arrangements.

As shown in figure 10(a), at a Mach number of 0.50 and for angles of attack of 12° and 16° , somewhat higher local velocities occurred around 17-percent chord on the upper surface of the airfoil when the slats were deflected to positions D or F than occurred with the slat retracted. This appears to be primarily a function of the loading on the slat which carries over onto the airfoil. As shown in most of the pressure distributions in figure 10, the local pressure coefficients exceeded the critical value in the vicinity of the trailing edge of the slat, indicating the

occurrence of local supersonic velocities. The subsonic stream of air which passed through the gap had a decelerating effect on the local air flow. As may be seen in figure 10(c) at angles of attack of 6° and 8° , the local velocities downstream of the deflected slat were less than those on the airfoil with the slat retracted.

The orientation of the slat with respect to the airfoil determined the path followed by the boundary layer which developed on the upper surface of the slat. This boundary layer either flowed onto and mixed with the boundary layer on the upper surface of the airfoil or it may have been discharged as a wake passing above the airfoil. The former would tend to have occurred with the slat positions involving small or negative deflection angles and closed or very small gaps, such as with positions B and E. The slat boundary layer might be expected to have been shed as a wake removed from the airfoil surface when the slat was oriented so as to have larger deflection angles and larger gaps, as exemplified by positions D, F, and G. For these latter positions, the boundary layer present at low speeds on the upper surface of the airfoil at positive angles of attack might be assumed to have originated in the slot rather than at the slat leading edge. At higher speeds a sonic throat existed between the airfoil and the slat trailing edge. It is conceivable that an improvement in slat performance at supercritical speeds might have been realized by shaping the slot so to have discharged a supersonic jet whose velocity more nearly approximated the local air velocity leaving the upper surface of the slat. Generally speaking, however, the loading and camber effects of slats and the accompanying influences on chordwise pressure gradient provide a clearer and more direct approach to an understanding of slat behavior than does the consideration of boundary-layer energization from the air flowing through the gap.

Further research appears both necessary and desirable on slats and leading-edge chord extensions for high-speed use. Worthy of attention would be slats and leading-edge devices which involved less droop and correspondingly less camber than those suggested by existing design criteria (ref. 1). Attention should be directed at determining the effects of these leading-edge devices on wings of finite span in addition to assessing their influences on the airfoil section characteristics.

CONCLUDING REMARKS

The results of the investigation of a slat in several different positions on a two-dimensional NACA 64A010 airfoil may be summarized as follows:

Over the entire Mach number range from 0.25 to 0.85, the airfoil with the slat retracted was generally aerodynamically superior to any of the other airfoil-slat arrangements for section lift coefficients up to 0.60.

At the lower Mach numbers, the highest maximum section lift coefficients and the largest lift-drag ratios at high angles of attack were obtained with the slat extended forward but with its nose displaced below the extended chord line of the airfoil (positions E and F). At the higher Mach numbers, adverse aerodynamic changes resulted with those slat arrangements. These adverse changes which occurred at the higher Mach numbers consisted of large increases in section drag, increased angle of attack for zero lift, and increasingly negative section pitching moments.

For section lift coefficients above 0.80 and for the widest range of test Mach numbers, the best aerodynamic characteristics were obtained with the nose of the slat on the extended chord line of the airfoil (position D).

The increased maximum lifts and lift-drag ratios at the higher angles of attack which were obtained with the slats extended may be attributed primarily to the increased loading carried by the slat and the forward portion of the airfoil and to the greater pressure recovery on the upper surface of the airfoil. The energizing effect on the boundary layer on the upper surface of the airfoil which is often attributed to the stream of air flowing through the gap appeared to be of secondary importance in determining slat performance.

Ames Aeronautical Laboratory
National Advisory Committee for Aeronautics
Moffett Field, Calif., Jan. 20, 1954

REFERENCES

1. Moss, G. F.: Systematic Wind-Tunnel Tests with Slats on a 10 Per Cent Thick Symmetrical Wing Section (EQ 1040 Profile). British, ARC R. & M. 2705 (12,068), 1948. Issued as: RAE Aero 2294, 1948.
2. Kelly, John A., and Hayter, Nora-Lee F.: Lift and Pitching Moment at Low Speeds of the NACA 64A010 Airfoil Section Equipped with Various Combinations of a Leading-Edge Slat, Leading-Edge Flap, Split Flap, and Double Slotted Flap. NACA TN 3007, 1953.
3. Nuber, Robert J., and Cheesman, Gail A.: Two-Dimensional Wind-Tunnel Investigation of a 6-Percent Thick Symmetrical Circular-Arc Airfoil Section with Leading-Edge and Trailing-Edge High-Lift Devices Deflected in Combination. NACA RM L9G20, 1949.
4. Axelson, John A.: Longitudinal Stability and Control of High-Speed Airplanes with Particular Reference to Dive Recovery. NACA RM A7C24, 1947.

5. Loftin, Laurence K., Jr.: Theoretical and Experimental Data for a Number of NACA 6A-Series Airfoil Sections. NACA Rep. 903, 1948. Issued as: NACA RM L6J01, 1946. (Formerly NACA TN 1368).
6. Millikan, Clark B.: Aerodynamics of the Airplane. John Wiley and Sons, Inc., 1941 pp. 85-86.

TABLE I.- SLAT RETRACTED, POSITION A

M	α	c_l	c_d	c_m	M	α	c_l	c_d	c_m	M	α	c_l	c_d	c_m	M	α	c_l	c_d	c_m			
0.25	-4	-0.414	0.018	-0.021	0.50	-1	-0.115	0.011	-0.007	0.70	-4	-0.547	0.024	-0.035	0.78	0	-0.033	0.012	-0.005			
	-3	-.296	.018	-.015		0	-.006	.011	-.002		-3	-.405	.017	-.024		1	.134	.015	.002			
	-2	-.204	.017	-.012		1	.098	.012	.003		-2	-.304	.014	-.017		2	.301	.020	.009			
	-1	-.096	.013	-.005		2	.221	.014	.008		-1	-.151	.010	-.009		3	.423	.027	.016			
	0	.009	.012	-.003		3	.318	.016	.013		0	-.006	.009	-.003		4	.550	.041	.021			
	1	.095	.013	.002		4	.445	.020	.019		1	.135	.011	.004		5	.638	.062	.022			
	2	.207	.015	.007		5	.551	.024	.025		2	.280	.013	.011		6	.691	.079	.021			
	3	.290	.017	.010		6	.642	.029	.032		3	.401	.017	.018		8	.816	.130	.016			
	4	.392	.020	.015		8	.773	.062	.043		4	.559	.026	.032		0.80	4	-.500	.046	-.020		
	5	.501	.023	.020		10	.800	.121	.019		5	.686	.041	.043			3	-.439	.034	-.021		
	6	.583	.027	.025		12	.847	.174	-.002		6	.719	.059	.042			2	-.349	.025	-.017		
	8	.792	.040	.034		14	.869	.216	-.014		8	.739	.104	.027			1	-.177	.018	-.007		
	10	.945	.058	.039		16	.893	.259	-.022		9	.783	.137	.015			0	-.031	.015	-.006		
	12	.918	.141	.013		0.60	-4	-.499	.018		-.028	0.72	-4	-.580			.027	-.039	1	.139	.017	-.001
	14	.933	.201	-.003			-3	-.374	.016		-.020		-3	-.437			.019	-.027	2	.293	.023	.005
	16	.841	.227	-.031			-2	-.277	.014		-.014		-2	-.325			.015	-.018	3	.389	.032	.009
	18	.743	.288	-.054			-1	-.135	.012		-.008		-1	-.176			.011	-.010	4	.504	.049	.014
	20	.815	.342	-.065			0	-.014	.011		-.003		0	-.019			.010	-.003	5	.586	.070	.014
0.40	-4	-.433	.016	-.021	1		.112	.012	.003	1	.127		.011	.004	0.82	4	-.459	.054	-.018			
	-3	-.315	.016	-.016	2		.239	.014	.009	2	.290		.014	.011		3	-.394	.039	-.017			
	-2	-.231	.014	-.011	3		.349	.017	.015	3	.417		.019	.018		2	-.324	.029	-.015			
	-1	-.108	.012	-.007	4		.485	.022	.022	4	.580		.028	.034		1	-.167	.025	-.007			
	0	-.001	.011	-.002	5		.596	.027	.031	5	.691		.047	.040		0	-.038	.021	-.007			
	1	.103	.012	.002	6		.675	.036	.040	6	.752		.063	.041		1	.121	.023	-.004			
	2	.214	.014	.007	8		.781	.080	.041	8	.759		.114	.030		2	.253	.028	.002			
	3	.302	.016	.011	10		.809	.133	.018	0.75	-4		-.573	.033	-.036	0.85	4	-.330	.079	-.064		
	4	.416	.020	.015	12		.835	.188	-.006		-3		-.455	.022	-.030		3	-.274	.055	-.039		
	5	.520	.024	.021	0.65	-4	-.500	.019	-.031		-2	-.345	.017	-.019	2		-.223	.046	-.034			
	6	.608	.028	.026		-3	-.375	.014	-.021		-1	-.185	.012	-.011	1		-.147	.041	-.016			
	8	.789	.049	.039		-2	-.272	.012	-.015		0	-.035	.010	-.004	0		-.016	.038	-.015			
	10	.824	.107	.027		-1	-.131	.010	-.009		1	.141	.012	.003	1		.055	.038	.010			
	12	.874	.161	.004		0	-.007	.009	-.003		2	.301	.016	.011	2		.140	.041	.013			
	14	.880	.209	-.009		1	.128	.010	.004		3	.411	.021	.017	3		.227	.053	.017			
	16	.880	.246	-.020		2	.266	.012	.010		4	.588	.034	.031	4		.330	.071	.023			
	18	.718	.266	-.043		3	.365	.015	.015		5	.663	.051	.032	NACA							
	20	.824	.348	-.067		4	.520	.021	.025	6	.726	.070	.032									
0.50	-4	-.462	.015	-.022		5	.626	.030	.037	0.78	-4	-.549	.041	-.027								
	-3	-.341	.014	-.017		6	.700	.045	.042		-3	-.471	.026	-.029								
	-2	-.245	.013	-.013		8	.752	.088	.031		-2	-.359	.021	-.019								
						10	.802	.143	.014		-1	-.183	.015	-.010								

TABLE II.- SLAT POSITION B

M	α	c_l	c_d	c_m	M	α	c_l	c_d	c_m	M	α	c_l	c_d	c_m	M	α	c_l	c_d	c_m
0.25	-4	-0.599	0.047	-0.063	0.40	10	0.830	0.127	0.086	0.60	4	0.489	0.043	0.060	0.72	1	-0.036	0.022	-0.023
	-3	-.469	.039	-.067		12	.883	.183	.060		5	.588	.063	.078		2	.141	.019	-.001
	-2	-.379	.035	-.056		14	.871	.233	.042		6	.674	.080	.090		3	.499	.052	.069
	-1	-.265	.029	-.046		16	.706	.246	.008		8	.771	.134	.077		4	.599	.067	.087
	0	-.142	.023	-.032		18	.778	.290	.005		10	.846	.185	.053					
	1	-.045	.020	-.020		20	.846	.354	0						0.75	-2	-.484	.045	-.080
	2	.058	.018	-.008						0.65	-4	-.639	.056	-.092		-1	-.364	.036	-.064
	3	.151	.017	.004	0.50	-4	-.636	.048	-.083		-3	-.561	.047	-.085		0	-.194	.026	-.043
	4	.252	.017	.015		-3	-.516	.043	-.071		-2	-.447	.038	-.071		1	-.159	.022	-.019
	5	.340	.018	.025		-2	-.425	.036	-.060		-1	-.322	.029	-.054		2	.138	.021	-.002
	6	.448	.023	.040		-1	-.300	.028	-.046		0	-.166	.022	-.035		3	.531	.054	.074
	8	.686	.036	.064		0	-.166	.023	-.031		1	-.036	.020	-.020	0.78	-1	-.390	.039	-.071
	10	.792	.087	.089		1	-.085	.020	-.027		2	.113	.018	-.003		0	-.211	.027	-.047
	12	.904	.128	.085		2	.072	.018	-.004		3	.431	.037	.053		1	-.057	.024	-.028
	14	.963	.191	.059		3	.187	.018	.010		4	.526	.054	.071		2	.126	.023	.006
	16	.937	.234	.043		4	.310	.020	.024		5	.622	.070	.086		3	.536	.059	.076
	18	.885	.270	.006		5	.515	.039	.058		6	.696	.089	.095	0.80	-1	-.412	.044	-.079
	20	.871	.305	.004		6	.599	.060	.074		8	.749	.139	.073		0	-.251	.032	-.054
0.40	-4	-.616	.046	-.077	0.60	8	.732	.099	.087	0.70	-3	-.574	.017	-.087		1	-.087	.026	-.035
	-3	-.496	.041	-.069		10	.816	.160	.068		-2	-.473	.018	-.076		2	.091	.028	-.005
	-2	-.397	.034	-.058		12	.823	.190	.050		-1	-.339	.018	-.058	0.82	0	-.274	.035	-.061
	-1	-.286	.028	-.045		14	.736	.225	.020		0	-.256	.020	-.036		1	-.097	.030	-.040
	0	-.158	.023	-.031							1	-.031	.023	-.023		2	.065	.031	.021
	1	-.053	.019	-.020		-4	-.661	.054	-.094		2	.144	.019	-.001	0.85	0	-.274	.035	-.061
	2	.060	.018	-.007		-3	-.541	.044	-.082		3	.490	.049	.066		1	-.097	.030	-.040
	3	.161	.018	.005		-2	-.450	.039	-.069		4	.579	.063	.082		2	.065	.031	.021
	4	.272	.019	.018		-1	-.325	.029	-.053		5	.648	.076	.090	0.72	-2	-.486	.044	-.079
	5	.390	.022	.030		0	-.174	.023	-.035		-2	-.486	.044	-.079		-1	-.351	.033	-.061
	6	.492	.027	.044		1	-.049	.020	-.021		-1	-.351	.033	-.061		0	.185	.025	.040
	8	.717	.076	.085		2	.094	.019	.005		0								
						3	.238	.018	.014										

NACA

TABLE III.- SLAT POSITION C

M	α	c_l	c_d	c_m	M	α	c_l	c_d	c_m	M	α	c_l	c_d	c_m	M	α	c_l	c_d	c_m	
0.25	-4	-0.541	0.045	-0.040	0.50	-1	-0.213	0.024	-0.030	0.70	-4	-0.541	0.061	-0.066	0.78	1	-0.050	0.022	-0.018	
	-3	-.400	.036	-.051		0	-.091	.019	-.016		-3	-.465	.051	-.063		2	.129	.021	.002	
	-2	-.320	.030	-.044		1	.029	.016	.004		-2	-.379	.040	-.054		3	.471	.043	.044	
	-1	-.213	.022	-.033		2	.141	.015	.009		-1	-.259	.030	-.041		4	.590	.061	.057	
	0	-.087	.014	-.019		3	.242	.016	.017		0	-.119	.022	-.023		5	.715	.082	.074	
	1	-.006	.012	-.008		4	.465	.024	.040		1	.026	.018	-.008		6	.798	.107	.074	
	2	.104	.010	.001		5	.576	.028	.054		2	.283	.019	.024	0.80	-4	-.494	.072	-.062	
	3	.192	.010	.011		6	.679	.049	.072		3	.482	.031	.050		-3	-.426	.057	-.061	
	4	.280	.014	.019		8	.824	.092	.097		4	.617	.048	.071		-2	-.361	.046	-.058	
	5	.398	.016	.027		10	.863	.136	.092		5	.722	.062	.091		-1	-.229	.033	-.041	
	6	.487	.019	.039		12	.903	.183	.081		6	.840	.085	.117		0	-.094	.026	-.024	
	8	.717	.028	.059		14	.950	.237	.066		0.72	-4	-.546	.067		-.066	1	.066	.024	.008
	10	.919	.040	.081		0.60	-4	-.552	.047	-.066		-3	-.474	.053	-.064	2	.279	.027	.028	
	12	.931	.100	.096			-3	-.442	.042	-.057		-2	-.390	.041	-.056	3	.372	.040	.034	
	14	.980	.151	.086			-2	-.352	.035	-.048		-1	-.269	.031	-.043	4	.473	.056	.038	
	16	1.048	.205	.078			-1	-.238	.026	-.035		0	-.120	.023	-.024	5	.605	.077	.052	
	18	1.040	.262	.056			0	-.101	.020	-.019		1	.018	.018	-.009	6	.690	.099	.061	
	20	1.020	.292	.054			1	.028	.017	-.005	2	.326	.022	.032	0.82	-4	-.491	.077	-.053	
0.40	-4	-.542	.045	-.051	0.65	2	.170	.015	.012	0.75	-4	-.535	.071	-.062		-3	-.404	.060	-.053	
	-3	-.406	.023	-.050		3	.395	.022	.034		-3	-.479	.060	-.065		-2	-.329	.047	-.052	
	-2	-.311	.026	-.042		4	.545	.031	.056		-2	-.401	.046	-.060		-1	-.200	.034	-.050	
	-1	-.202	.026	-.031		5	.658	.049	.073		-1	-.292	.034	-.046		0	-.059	.029	-.036	
	0	-.084	.018	-.018		6	.736	.066	.088		0	-.146	.025	-.028		1	.098	.026	-.006	
	1	.012	.014	-.006		8	.844	.102	.105		1	.015	.020	-.012	2	.283	.034	.029		
	2	.115	.014	.005		10	.864	.157	.088		2	.320	.023	.034	3	.353	.045	.030		
	3	.213	.014	.014		0.55	-4	-.529	.052	-.092	3	.507	.039	.053	4	.455	.063	.035		
	4	.308	.016	.023			-3	-.427	.043	-.079	4	.648	.058	.076	5	.573	.083	.046		
	5	.415	.019	.030			-2	-.334	.036	-.068	5	.763	.075	.091	6	.662	.107	.048		
	6	.528	.024	.043			-1	-.226	.027	-.049	0.78	-4	-.498	.074	-.064	0.85	-3	-.294	.084	-.088
	8	.778	.062	.080			0	-.096	.021	-.019		-3	-.501	.077	-.065		-2	-.222	.066	-.073
	10	.876	.111	.098			1	.037	.017	-.005		-2	-.436	.054	-.066		-1	-.159	.049	-.048
	12	.918	.157	.089			2	.188	.015	.013		0	-.345	.040	-.053		0	-.110	.045	-.031
	14	.974	.209	.073			3	.433	.024	.062		1	-.301	.077	-.065		1	.034	.040	-.005
	16	.981	.265	.057			4	.563	.038	.088		2	-.436	.054	-.066		2	.221	.048	.034
	18	.975	.309	.052			5	.655	.056	.112		-1	-.345	.040	-.053		3	.265	.061	.040
	20	.978	.352	.040			6	.747	.073	.095		0	-.196	.028	-.035		4	.382	.077	.035
0.50	-4	-.523	.042	-.062		8	.824	.113	.102											
	-3	-.407	.037	-.051		9	.836	.144	.094											
	-2	-.322	.031	-.042																

NACA

TABLE IV.- SLAT POSITION D

M	α	σ_1	σ_d	σ_m	M	α	σ_1	σ_d	σ_m	M	α	σ_1	σ_d	σ_m	M	α	σ_1	σ_d	σ_m			
0.25	-4	-0.415	0.028	-0.036	0.50	1	0.035	0.022	-0.006	0.70	-1	-0.196	0.022	-0.022	0.78	2	0.153	0.028	0.002			
	-3	-.294	.026	-.026		2	.164	.022	.001		0	-.074	.020	-.010		3	.296	.033	.009			
	-2	-.225	.021	-.017		3	.265	.023	.008		1	.014	.023	-.006		4	.418	.046	.015			
	-1	-.123	.019	-.012		4	.387	.025	.016		2	.163	.025	.001		5	.552	.063	.023			
	0	-.050	.021	-.012		5	.523	.029	.027		3	.302	.027	.011		6	.635	.073	.031			
	1	.041	.020	-.008		6	.647	.034	.040		4	.444	.031	.021		8	.870	.121	.044			
	2	.148	.021	-.002		8	.886	.051	.068		5	.613	.041	.038		0.80	-4	-.518	.066	-.049		
	3	.235	.021	.004		10	1.038	.099	.092		6	.735	.054	.053			-3	-.431	.049	-.048		
	4	.355	.023	.013		12	1.135	.130	.108		8	.978	.093	.087			-2	-.333	.037	-.039		
	5	.465	.026	.022		14	1.185	.184	.105		9	1.063	.125	.098			-1	-.212	.028	-.025		
	6	.577	.029	.030		16	1.191	.231	.098		0.72	-4	-.503	.055	-.057		0	-.088	.023	-.011		
	8	.797	.041	.049		0.60	-4	-.499	.038	-.051		-3	-.408	.038	-.045		1	.016	.027	-.003		
	10	1.005	.054	.069			-3	-.374	.030	-.038		-2	-.326	.030	-.035		2	.146	.031	.002		
	12	1.159	.071	.081			-2	-.288	.025	-.028		-1	-.196	.023	-.022		3	.264	.036	.007		
	14	1.203	.144	.099			-1	-.166	.021	-.016		0	-.072	.020	-.010		4	.402	.052	.013		
	16	1.267	.181	.104			0	-.083	.020	-.009		1	.020	.023	-.005		5	.493	.066	.019		
	18	1.267	.245	.091			1	.014	.022	-.006		2	.165	.026	.002		6	.588	.081	.022		
	20	1.271	.301	.077			2	.138	.023	-.001		3	.307	.028	.011		8	.804	.125	.027		
0.40	-4	-.418	.029	-.037	0.65		3	.264	.024	.007		0.75	-4	-.513	.057	-.059	0.82	-4	-.480	.070	-.042	
	-3	-.309	.025	-.027			4	.413	.027	.018			5	.613	.046	.036		-3	-.401	.051	-.043	
	-2	-.230	.022	-.019			5	.568	.031	.031			6	.721	.058	.050		-2	-.324	.042	-.037	
	-1	-.128	.019	-.011			6	.693	.038	.046			8	.991	.101	.085		-1	-.195	.031	-.022	
	0	-.065	.020	-.010			8	.919	.070	.077			9	1.038	.126	.091		0	-.083	.027	-.010	
	1	.031	.021	-.007			10	1.073	.110	.104	0.78		-4	-.534	.061	-.060		1	-.005	.044	.007	
	2	.143	.021	0			12	1.156	.154	.110			-3	-.411	.040	-.047		2	.067	.048	.017	
	3	.247	.021	.007		0.70	-4	-.502	.047	-.054			-2	-.325	.031	-.037		3	.138	.053	.019	
	4	.346	.023	.013			-3	-.397	.032	-.044			-1	-.200	.024	-.024		4	.252	.066	.022	
	5	.475	.027	.023			-2	-.310	.026	-.034			0	-.081	.020	-.010		5	.374	.084	.022	
	6	.588	.030	.040			-1	-.186	.021	-.021			1	.014	.023	-.005		0.85	-4	-.399	.083	-.055
	8	.822	.045	.055			0	-.081	.019	-.010			2	.160	.026	.002			-3	-.337	.062	-.045
	10	.999	.083	.079			1	.013	.022	-.007		3	.300	.029	.010	-2	-.285		.050	-.039		
	12	1.110	.116	.096			2	.129	.023	-.002		4	.466	.039	.022	-1	-.172		.043	-.024		
	14	1.189	.164	.104			3	.257	.024	.006		5	.577	.051	.028	0	-.071		.039	-.011		
	16	1.221	.203	.101			4	.412	.028	.017		6	.686	.067	.040	1	-.005		.044	.007		
	18	1.217	.275	.082			5	.569	.035	.031		8	.939	.110	.066	2	.067		.048	.017		
	20	1.212	.322	.064			6	.685	.044	.045	0.78	-4	-.534	.061	-.060	3	.138		.053	.019		
0.50	-4	-.452	.034	-.041	8		.936	.077	.080	-3		-.424	.044	-.050	4	.252	.066		.022			
	-3	-.336	.026	-.029	10	1.100	.125	.106	-2	-.329		.035	-.039	5	.374	.084	.022					
	-2	-.255	.022	-.020	0.70	-4	-.504	.053	-.055	-1		-.210	.026	-.025								
	-1	-.142	.019	-.011		-3	-.404	.036	-.044	0		-.088	.021	-.011								
	0	-.064	.021	-.009		-2	-.324	.028	-.035	1		-.008	.024	-.003								

NACA

TABLE V.- SLAT POSITION E

M	α	c_l	c_d	c_m	M	α	c_l	c_d	c_m	M	α	c_l	c_d	c_m	M	α	c_l	c_d	c_m
0.25	-4.5	-0.502	0.045	-0.110	0.40	15.5	1.206	0.139	0.100	0.60	5.5	0.542	0.031	-0.012	0.72	0.5	-0.158	0.068	-0.105
	-2.5	-.324	.032	-.094		17.5	1.187	.235	.066		7.5	.745	.045	.024		1.5	-.064	.060	-.096
	-0.5	-.094	.025	-.072		19.5	1.174	.253	.065		9.5	1.069	.086	.050		2.5	.057	.056	-.080
	1.5	.132	.020	-.043												3.5	.185	.050	-.064
	3.5	.347	.021	-.021	0.50	-4.5	-.463	.117	-.053	0.65	-4.5	-.435	.132	-.053	0.75	4.5	.317	.046	-.051
	5.5	.561	.027	.001		-3.5	-.443	.101	-.068		-3.5	-.436	.114	-.066		5.5	.409	.046	-.042
	7.5	.778	.038	.024		-2.5	-.424	.084	-.080		-2.5	-.418	.100	-.076		7.5	.625	.072	-.013
	9.5	.978	.048	.050		-1.5	-.367	.066	-.093		-1.5	-.350	.080	-.090		9.5	.874	.125	-.025
	11.5	1.155	.065	.071		-0.5	-.211	.036	-.088		-0.5	-.257	.064	-.097					
	13.5	1.280	.087	.085		0.5	-.108	.030	-.075		0.5	-.150	.049	-.090		2.5	.035	.058	-.088
	15.5	1.395	.125	.100		1.5	.022	.026	-.061		1.5	-.026	.036	-.077		3.5	.143	.058	-.078
	17.5	1.395	.180	.094		2.5	.153	.024	-.047		2.5	.110	.028	-.065		4.5	.234	.057	-.070
	19.5	1.300	.273	.048		3.5	.282	.023	-.033		3.5	.256	.026	-.047		5.5	.351	.059	-.057
						4.5	.416	.020	-.018		4.5	.399	.031	-.031		7.5	.576	.081	-.023
0.40	-4.5	-.482	.102	-.059	0.60	5.5	.525	.027	-.006	0.70	-4.5	-.420	.137	-.054	0.78	9.5	.756	.122	-.001
	-3.5	-.439	.085	-.079		7.5	.776	.039	.024		-3.5	-.406	.119	-.062					
	-2.5	-.394	.064	-.097		9.5	.968	.055	.064		-2.5	-.397	.109	-.068		2.5	-.012	.055	-.101
	-1.5	-.275	.036	-.092		11.5	1.135	.094	.096		-1.5	-.337	.074	-.092		3.5	.078	.059	-.093
	-0.5	-.177	.030	-.080							-0.5	-.280	.070	-.099	0.80	4.5	.171	.060	-.080
	0.5	-.077	.027	-.069		-4.5	-.418	.123	-.051		0.5	-.184	.059	-.099		5.5	.264	.063	-.067
	1.5	.051	.023	-.053		-3.5	-.418	.106	-.064		1.5	-.048	.048	-.088		7.5	.475	.085	-.043
	2.5	.183	.023	-.041		-2.5	-.399	.093	-.075		2.5	.082	.037	-.071	0.82	9.5	.709	.124	-.014
	3.5	.300	.021	-.029		-1.5	-.337	.074	-.092		3.5	.208	.033	-.056					
	4.5	.426	.022	-.015		-0.5	-.297	.056	-.094		4.5	.348	.037	-.041		4.5	.112	.070	-.093
	5.5	.527	.025	-.005		0.5	-.133	.041	-.087		5.5	.454	.044	-.032		5.5	.214	.075	-.076
	7.5	.761	.036	.024	0.70	1.5	-.011	.029	-.073		7.5	.672	.067	0		7.5	.408	.093	-.055
	9.5	.971	.047	.051		2.5	.121	.025	-.058										
	11.5	1.144	.062	.076		3.5	.271	.026	-.042							5.5	.109	.080	-.092
	13.5	1.195	.105	.096		4.5	.413	.026	-.025							7.5	.332	.098	-.064



TABLE VI.- SLAT POSITION F

16

M	α	c_l	c_d	c_m	M	α	c_l	c_d	c_m	M	α	c_l	c_d	c_m	M	α	c_l	c_d	c_m		
0.25	-4	-0.474	0.120	-0.030	0.50	-4	-0.402	0.118	-0.032	0.65	2	-0.026	0.047	-0.072	0.75	-4	-0.326	0.135	-0.050		
	-3	-.454	.104	-.052		-3	-.402	.107	-.042		3	.084	.038	-.060		-3	-.310	.118	-.055		
	-2	-.409	.088	-.067		-2	-.385	.095	-.053		4	.203	.032	-.046		-2	-.298	.105	-.061		
	-1	-.319	.071	-.075		-1	-.334	.080	-.062		5	.299	.032	-.032		-1	-.272	.092	-.068		
	0	-.204	.054	-.073		0	-.228	.062	-.073		6	.438	.037	-.017		0	-.223	.078	-.079		
	1	-.106	.041	-.066		1	-.121	.050	-.073		8	.704	.055	.012		1	-.147	.066	-.085		
	2	-.003	.027	-.056		2	-.029	.030	-.062		10	.989	.097	.044		2	-.053	.056	-.084		
	3	.091	.027	-.047		3	.074	.028	-.051		12	1.059	.124	.043		3	.073	.051	-.074		
	4	.195	.027	-.036		4	.182	.028	-.038		13	1.140	.150	.052		4	.200	.048	-.059		
	5	.292	.030	-.026		5	.291	.030	-.026		0.70	-4	-.331	.127		-.043	0.78	5	.286	.049	-.050
	6	.383	.033	-.015		6	.396	.033	-.013			-4	-.328	.114		-.048		6	.374	.054	-.043
	8	.600	.043	.004		8	.652	.043	.014			-3	-.311	.101		-.057		8	.496	.075	-.025
	10	.814	.047	.021		10	.925	.051	.040			-2	-.287	.087		-.067		10	.694	.114	-.002
	12	.997	.057	.038		12	1.178	.071	.073			-1	-.240	.073		-.074		-3	-.268	.132	-.065
	14	1.169	.079	.058		14	1.286	.105	.094			0	-.147	.060		-.082		-2	-.256	.116	-.067
	16	1.293	.097	.070		16	1.376	.157	.106			1	-.049	.050		-.079		-1	-.232	.097	-.075
	18	1.421	.123	.085		18	1.426	.213	.093			2	.074	.043		-.069		0	-.193	.084	-.084
	20	1.489	.256	.095		0.60	-4	-.359	.119			-.036	3	.209		.037		-.051	1	-.148	.072
0.40	-4	-.429	.124	-.028	-3		-.364	.108	-.045	4		.209	.037	-.051	2	-.071		.061	-.088		
	-3	-.426	.106	-.044	-2		-.348	.094	-.055	5		.307	.035	-.046	3	.037		.056	-.085		
	-2	-.398	.091	-.056	-1		-.303	.078	-.066	6		.433	.044	-.023	4	.138		.056	-.077		
	-1	-.340	.076	-.070	0		-.211	.061	-.076	8		.639	.066	-.004	5	.246		.059	-.066		
	0	-.227	.058	-.073	1		-.115	.047	-.076	10		.833	.109	.017	6	.325		.066	-.059		
	1	-.128	.043	-.070	2		.013	.041	-.066	12		1.067	.148	.023	8	.494		.087	-.045		
	2	-.026	.028	-.058	3		.110	.030	-.055	0.72		-4	-.325	.129	-.046	10		.724	.133	-.048	
	3	.074	.027	-.042	4		.219	.030	-.040			-4	-.319	.118	-.051	0.80		3	-.079	.071	-.099
	4	.173	.027	-.037	5		.341	.032	-.027			-3	-.301	.103	-.058			4	.006	.065	-.096
	5	.284	.029	-.026	6		.455	.036	-.012		-2	-.275	.089	-.068	5		.097	.064	-.087		
	6	.382	.032	-.016	8		.716	.049	.016		0	-.226	.074	-.077	6		.212	.071	-.074		
	8	.602	.041	.006	10		1.086	.081	.062		1	-.149	.062	-.083	7		.306	.077	-.064		
	10	.831	.047	.025	12		1.198	.107	.075		2	-.046	.052	-.080	8		.386	.088	-.057		
	12	1.045	.055	.049	13		1.268	.131	.088		3	.027	.042	-.068	10		.576	.122	-.047		
	14	1.224	.080	.074	0.65		-4	-.347	.124		-.038	4	.208	.040	-.054		0.82	5	.022	.068	-.097
	16	1.348	.124	.092			-3	-.346	.108		-.046	5	.311	.039	-.041			6	.151	.072	-.081
	18	1.398	.176	.100			-2	-.335	.097		-.053	6	.418	.045	-.031			7	.231	.083	-.071
	20	1.406	.238	.096		-1	-.295	.083	-.068		8	.559	.067	-.012	8			.388	.097	-.075	
				0		-.230	.069	-.076	10		.784	.115	.009	9	.419			.108	-.059		
				1		-.136	.057	-.079	11		.857	.136	.007	10	.517			.126	-.059		

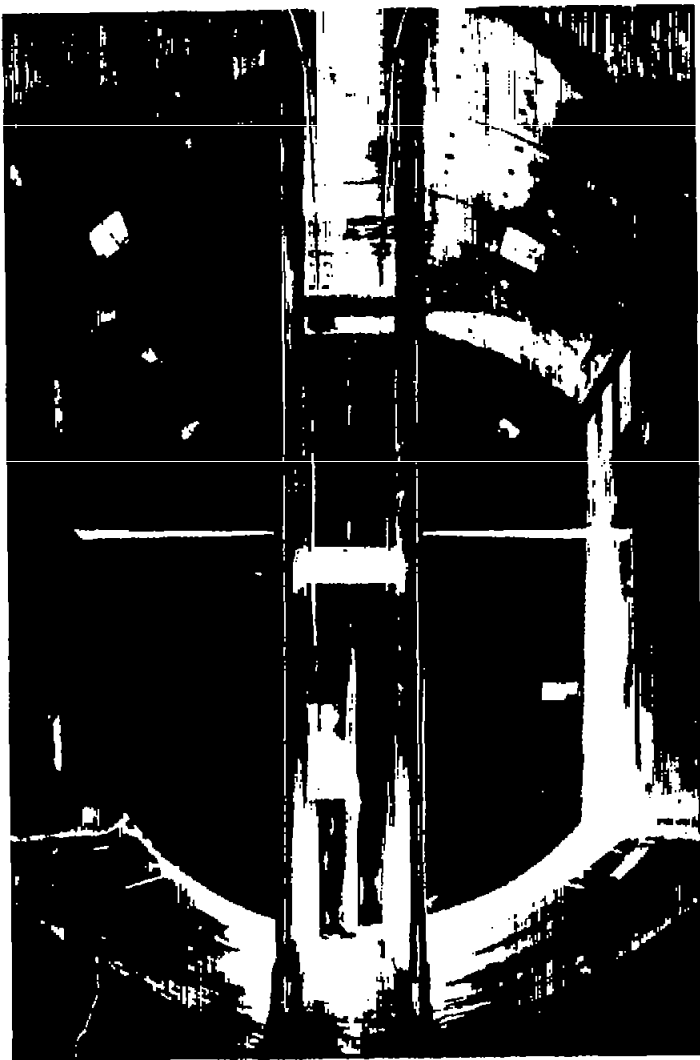
NACA

NACA TN 3129

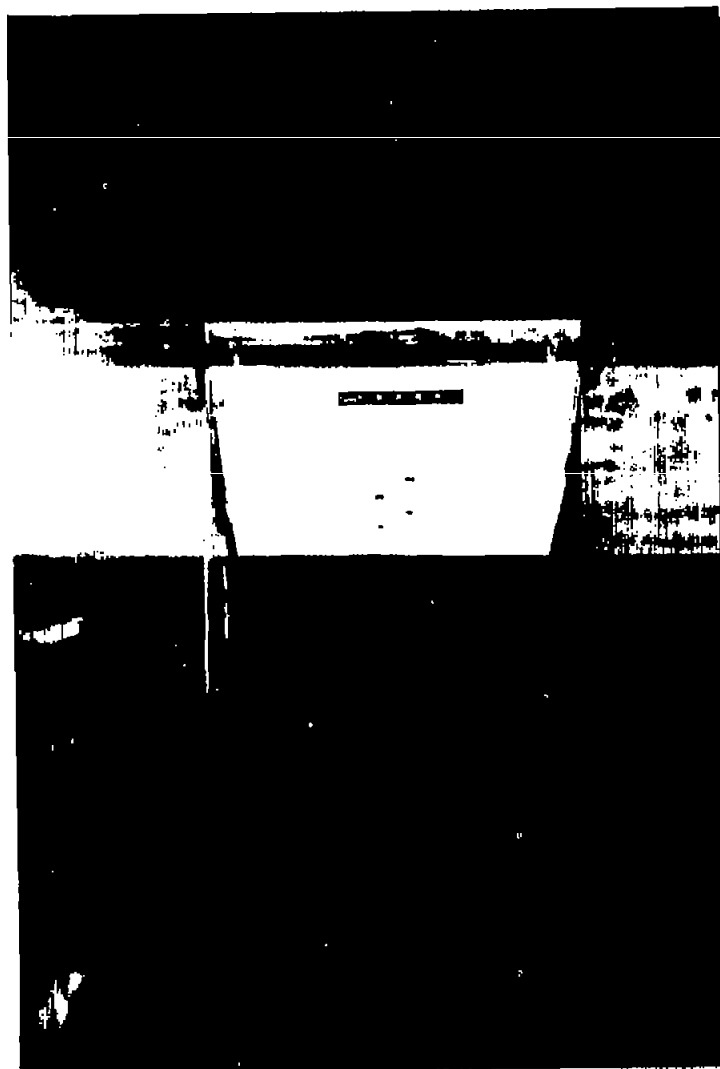
TABLE VII.- SLAT POSITION G

M	α	α_1	α_d	α_m	M	α	α_1	α_d	α_m	M	α	α_1	α_d	α_m	M	α	α_1	α_d	α_m			
0.25	-4	-0.442	0.136	-0.011	0.50	-1	-0.352	0.087	-0.050	0.65	4	0.080	0.054	-0.056	0.75	-1	-0.294	0.097	-0.062			
	-3	-.432	.117	-.029		0	-.286	.072	-.064		5	.155	.056	-.048		0	-.265	.087	-.070			
	-2	-.418	.105	-.043		1	-.189	.057	-.070		6	.238	.059	-.038		1	-.214	.076	-.078			
	-1	-.372	.088	-.060		2	-.101	.050	-.067		8	.421	.057	-.013		2	-.141	.068	-.081			
	0	-.289	.068	-.066		3	-.012	.046	-.059		10	.949	.096	-.007		3	-.048	.063	-.077			
	1	-.184	.053	-.069		4	.111	.043	-.044		12	.829	.125	-.001		4	.039	.063	-.069			
	2	-.091	.045	-.064		5	.182	.041	-.034		14	1.012	.169	-.026		5	.100	.066	-.062			
	3	-.001	.042	-.058		6	.273	.045	-.027		0.70	-4	-.345	.135		-.033	6	.133	.072	-.062		
	4	.101	.033	-.043		8	.488	.046	-.009			-3	-.344	.119		-.040	8	.284	.087	-.050		
	5	.180	.035	-.034		10	.731	.056	-.003			-2	-.337	.110		-.046	10	.515	.099	-.018		
	6	.265	.038	-.028		12	.880	.090	.004			-1	-.320	.096		-.057	12	.740	.143	-.022		
	8	.457	.042	-.016		14	1.092	.103	.034			0	-.276	.083		-.066	0.78	-2	-.274	.122	-.065	
	10	.652	.047	-.002		16	1.313	.123	.065			1	-.217	.072		-.075		-1	-.280	.106	-.070	
	12	.764	.065	-.006		18	1.277	.184	.046			2	-.128	.062		-.076		0	-.246	.093	-.079	
	14	.902	.087	-.004		20	1.346	.232	.054			3	-.034	.059		-.072		1	-.209	.083	-.084	
	16	1.055	.095	.014		0.60	-4	-.362	.132			-.025	4	.063		.059		-.063	2	-.144	.073	-.085
	18	1.190	.114	.028			-3	-.370	.119			-.032	5	.125		.061		-.055	3	-.065	.069	-.082
	20	1.322	.130	.037			-2	-.366	.107			-.041	6	.188		.067		-.050	4	.003	.067	-.074
0.40	-4	-.404	.130	-.017	-1		-.344	.094	-.052	8		.303	.076	-.037	5	.053		.070	-.070			
	-3	-.404	.118	-.027	0		-.292	.079	-.064	10		.649	.084	0	6	.097		.076	-.069			
	-2	-.397	.103	-.038	1		-.200	.066	-.072	12		.814	.139	-.010	8	.181		.097	-.055			
	-1	-.361	.086	-.053	2		-.114	.056	-.072	0.72		-4	-.336	.139	-.036	10		.364	.109	-.037		
	0	-.303	.073	-.063	3		-.015	.052	-.064			-3	-.334	.123	-.043	0.80		0	-.226	.105	-.089	
	1	-.199	.057	-.067	4		.097	.052	-.052			-2	-.332	.112	-.049			1	-.211	.093	-.088	
	2	-.114	.050	-.067	5		.184	.054	-.041			-1	-.304	.095	-.059			2	-.161	.080	-.090	
	3	-.020	.045	-.059	6		.248	.053	-.031		0	-.279	.084	-.068	3			-.098	.073	-.088		
	4	.094	.042	-.046	8		.455	.053	-.009		1	-.224	.071	-.075	4			-.030	.070	-.081		
	5	.168	.039	-.036	10		.794	.085	.002		2	-.138	.065	-.079	5			.008	.073	-.076		
	6	.255	.042	-.027	12		.853	.115	.001		3	-.040	.060	-.075	6			.052	.080	-.074		
	8	.453	.044	-.014	14		1.021	.141	.021		4	.051	.060	-.066	8		.200	.101	-.066			
	10	.671	.051	-.001	16		1.198	.180	.029		5	.119	.064	-.058	10		.413	.125	-.054			
	12	.784	.075	-.006	0.65		-4	-.355	.131		-.028	0.75	6	.161	.069		-.056	0.82	4	-.058	.078	-.094
	14	.911	.092	.001			-3	-.355	.117		-.034		8	.304	.082		-.041		5	.014	.079	-.082
	16	1.098	.108	.024		-2	-.349	.106	-.042		10		.598	.088	-.005		6		.028	.084	-.077	
	18	1.323	.139	.052		-1	-.331	.093	-.053		12		.781	.142	-.018		7		.090	.095	-.074	
	20	1.379	.195	.043		0	-.279	.078	-.065		-4		-.320	.141	-.040		8		.183	.108	-.069	
0.50	-4	-.380	.127	-.033		1	-.210	.067	-.072		-3		-.318	.126	-.047		9		.279	.120	-.066	
	-3	-.391	.116	-.028		2	-.114	.058	-.073		-2		-.313	.112	-.053							
	-2	-.382	.103	-.038		3	-.020	.054	-.067													



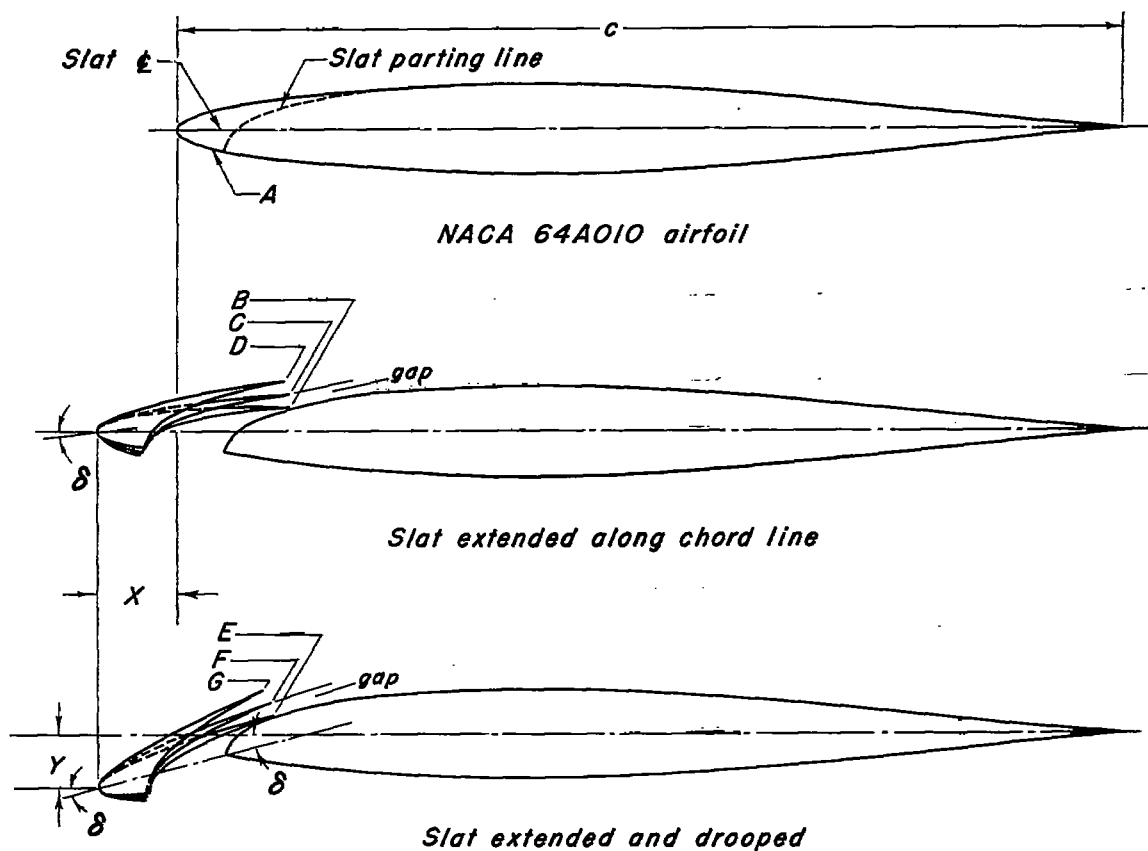


A-16842.1



A-16843.1

Figure 1.- Airfoil installed between the two-dimensional walls.



64A010 airfoil coordinates		Slat parting line	
x % chord	y % chord	x % chord	y % chord
0	0	4.70	-2.20
.50	.80	4.80	-1.85
.75	.97	5.00	-1.36
1.25	1.22	5.40	-0.69
2.50	1.69	6.00	-0.03
5.00	2.32	7.00	0.74
10.00	3.20	8.00	1.31
15.00	3.81	10.00	2.12
20.00	4.27	12.00	2.71
30.00	4.84	14.00	3.21
40.00	4.99	16.00	3.70
50.00	4.68	17.00	3.94
60.00	4.02		
70.00	3.12		
80.00	2.10		
90.00	1.06		
100.00	.02		
L.E.R = 0.688			

Slat position	$\frac{X}{c}$	$\frac{Y}{c}$	$\frac{gap}{c}$	δ	$\Delta \delta^*$
A	0	0	0 \pm 0*	0	0
B	.09	0	0 \pm .001	-8.4°	\pm 1.0°
C	.09	0	.015 \pm .002	-3.3°	\pm 1.0°
D	.09	0	.030 \pm .002	1.6°	\pm 1.0°
E	.09	.06	0 \pm .001	9.5°	\pm 1.0°
F	.09	.06	.015 \pm .002	14.5°	\pm 2.0°
G	.09	.06	.030 \pm .002	19.5°	\pm 2.0°

NACA

*These increments are the variations possible from the normal values due to bracket deflections, clearances, etc.

Figure 2.- Airfoil coordinates and slat details.

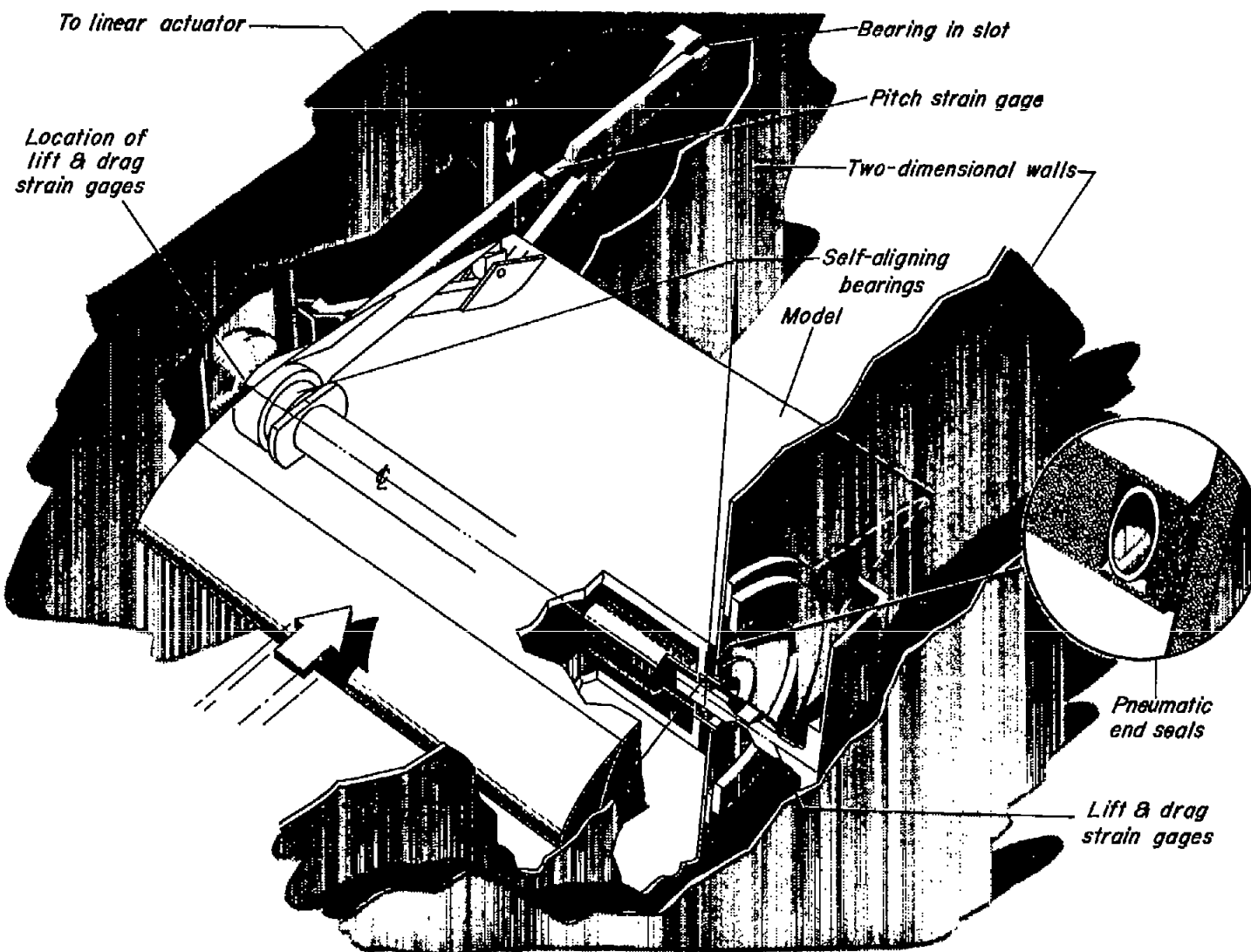


Figure 3.- Model support and strain-gage balance.

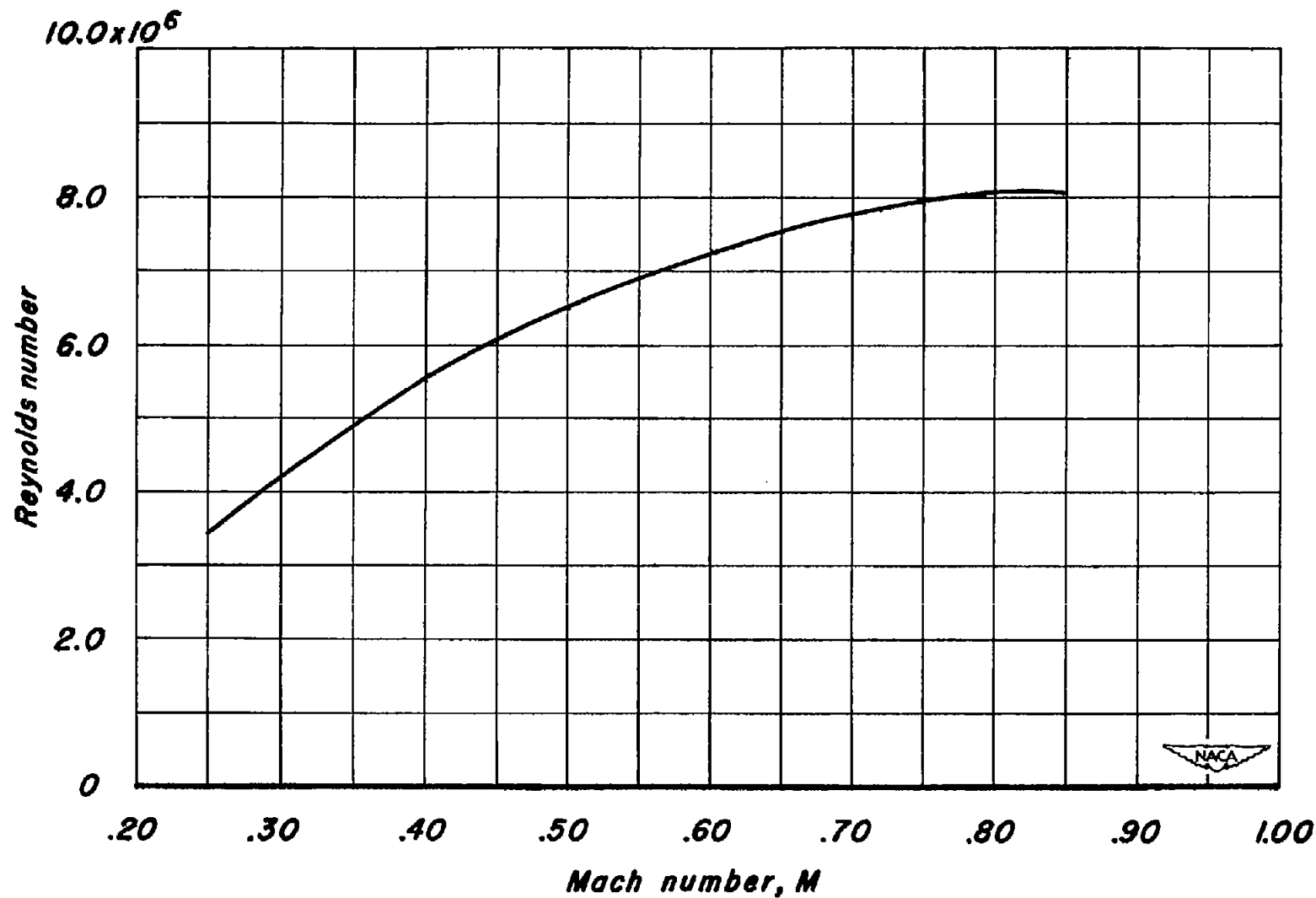


Figure 4.- Variation of Reynolds number with Mach number.

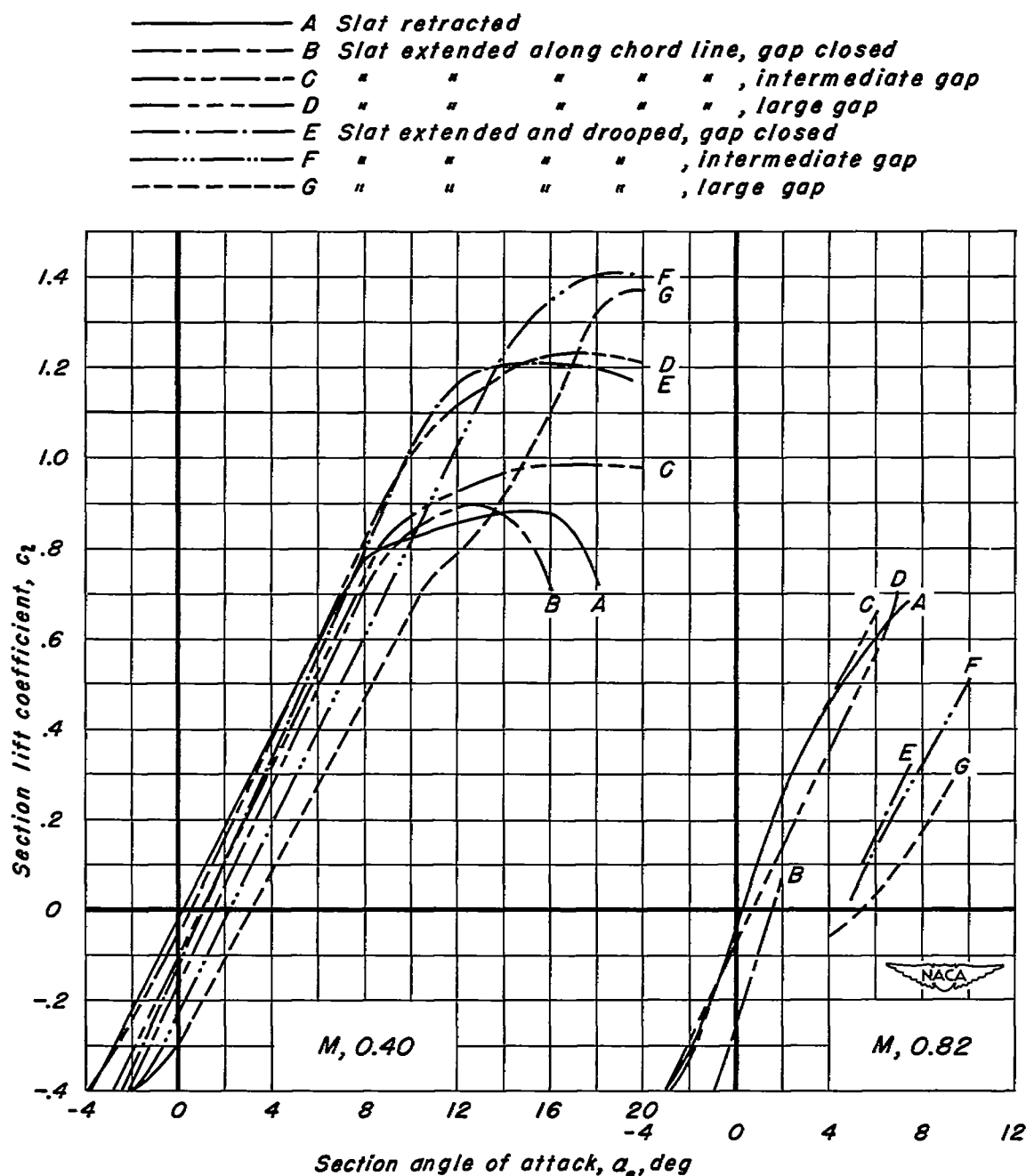


Figure 5.- Lift characteristics of the NACA 64A010 airfoil with several slat positions at low and high subsonic Mach numbers.

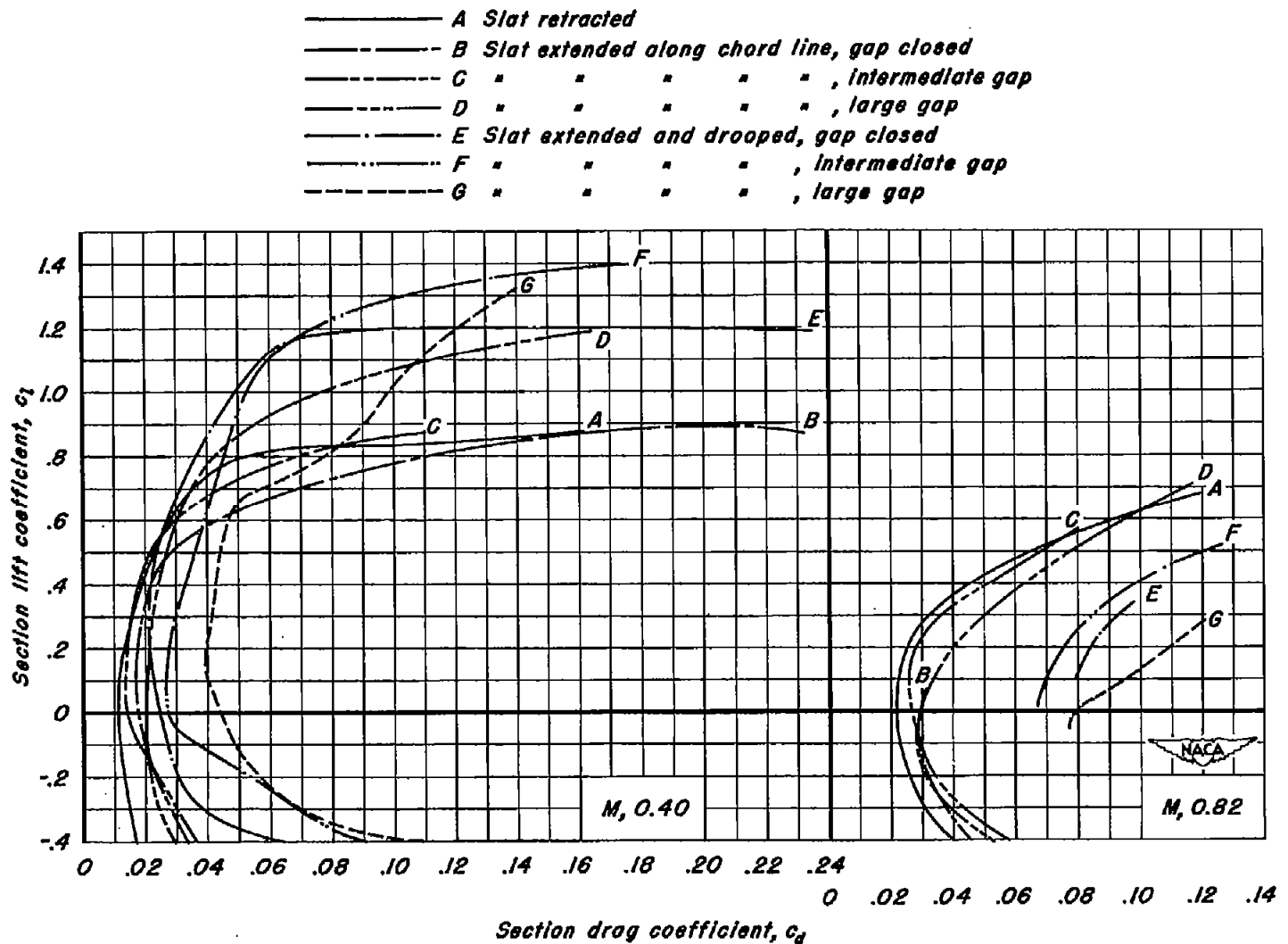


Figure 6.- Drag characteristics of the NACA 64A010 airfoil with several slat positions at low and high subsonic Mach numbers.

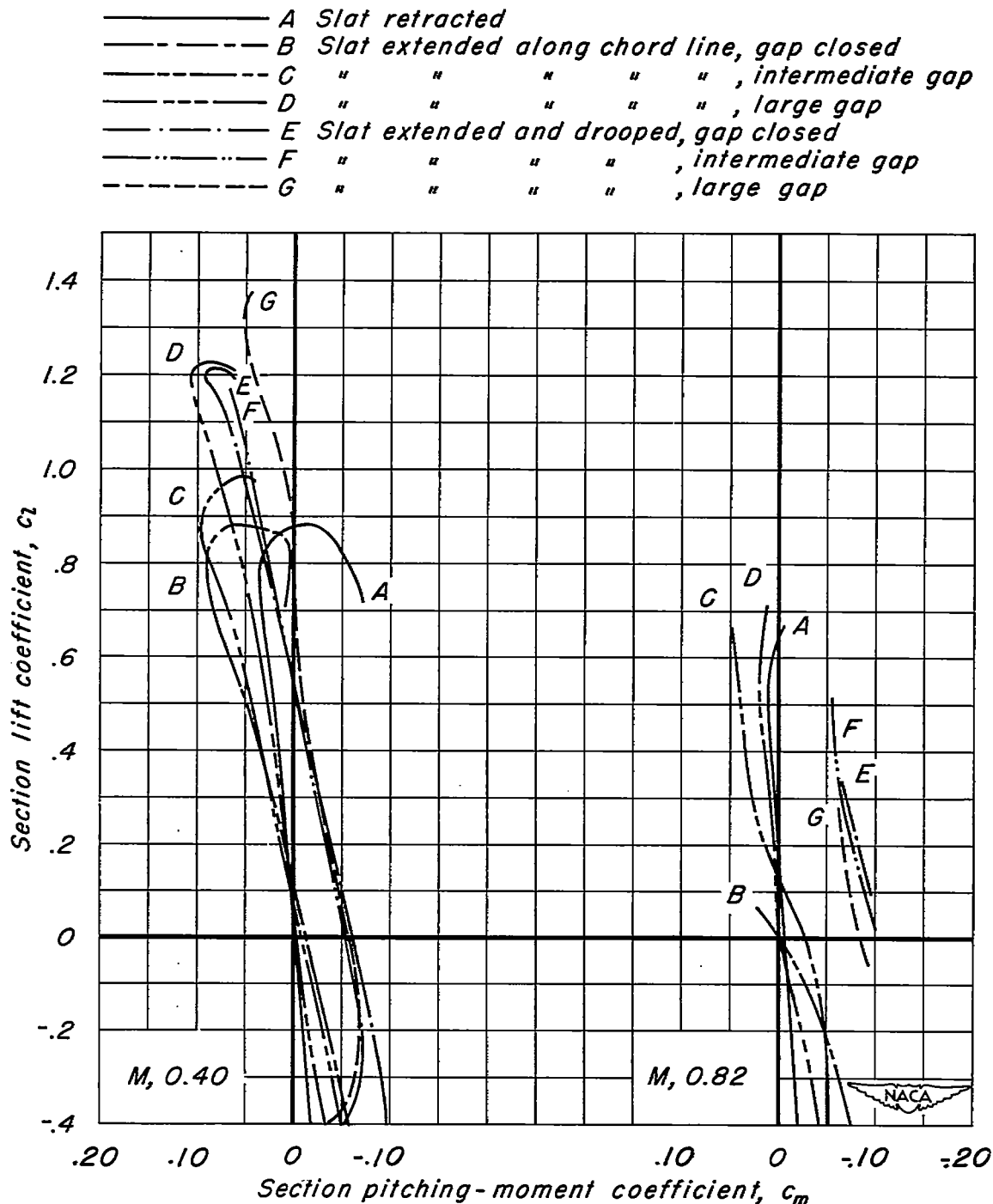
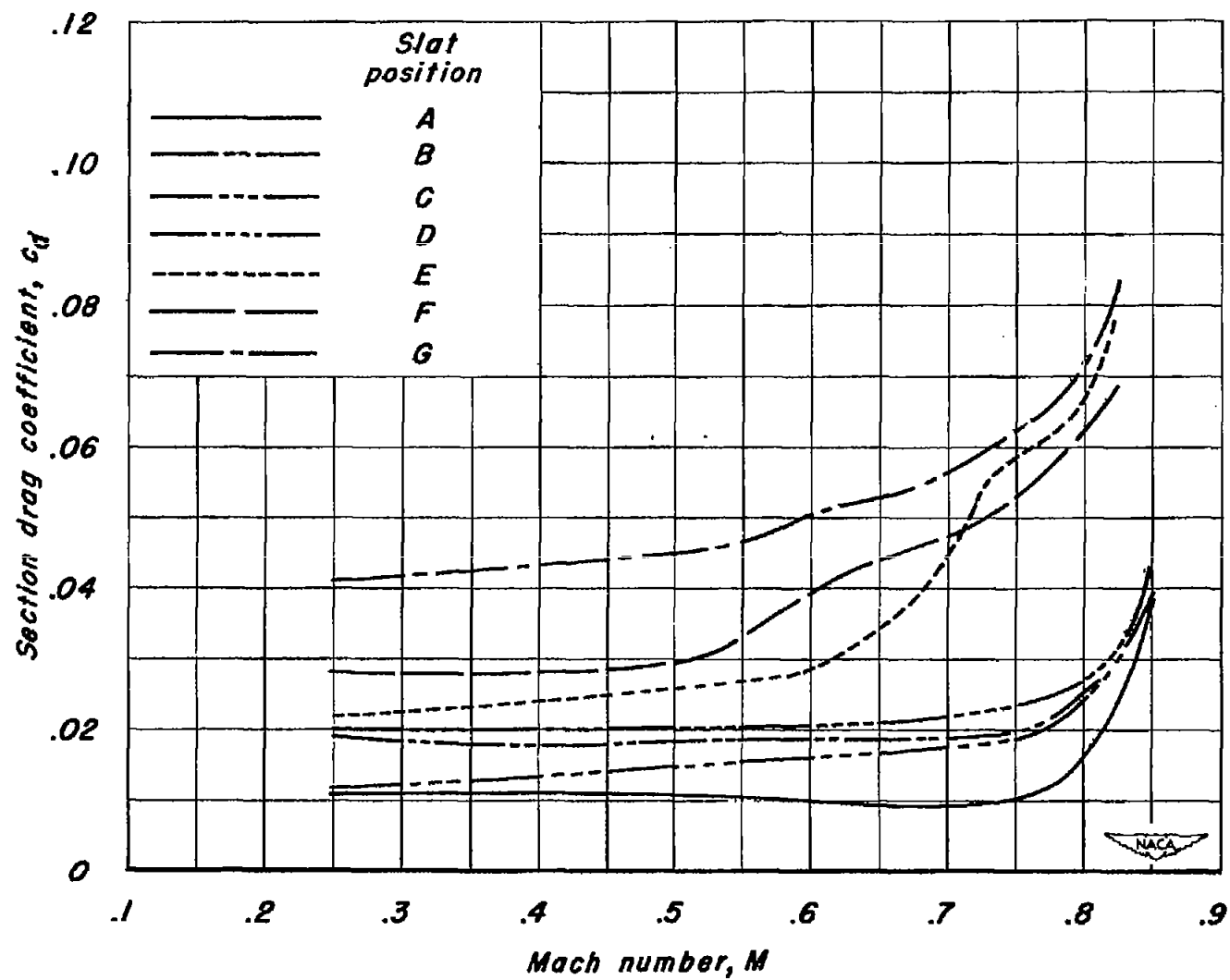


Figure 7.- Variation of section pitching-moment coefficient with section lift coefficient for the NACA 64A010 airfoil with several slat positions at low and high subsonic Mach numbers.



(a) $c_l, 0$.

Figure 8.- Variation of section drag coefficient with Mach number.

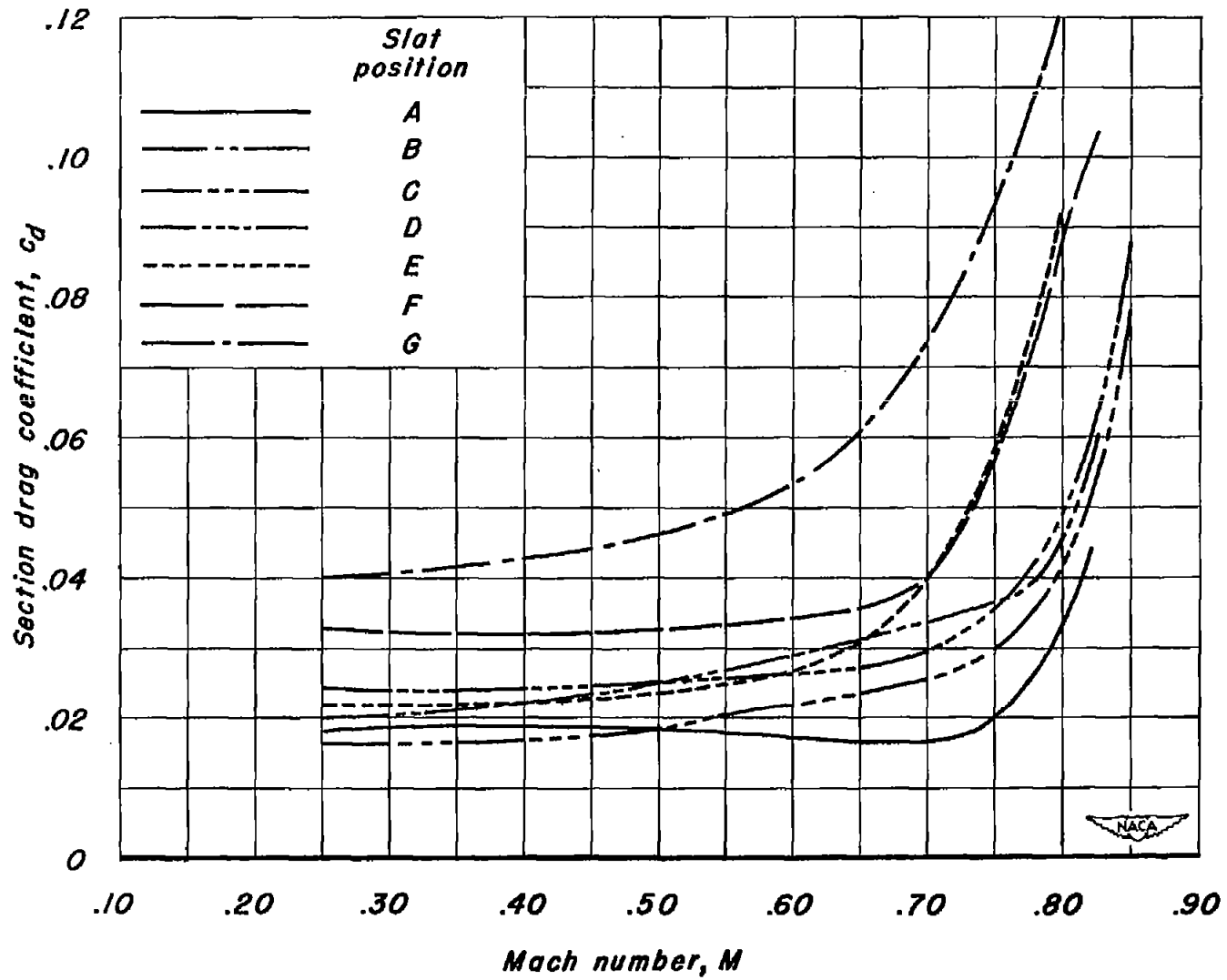
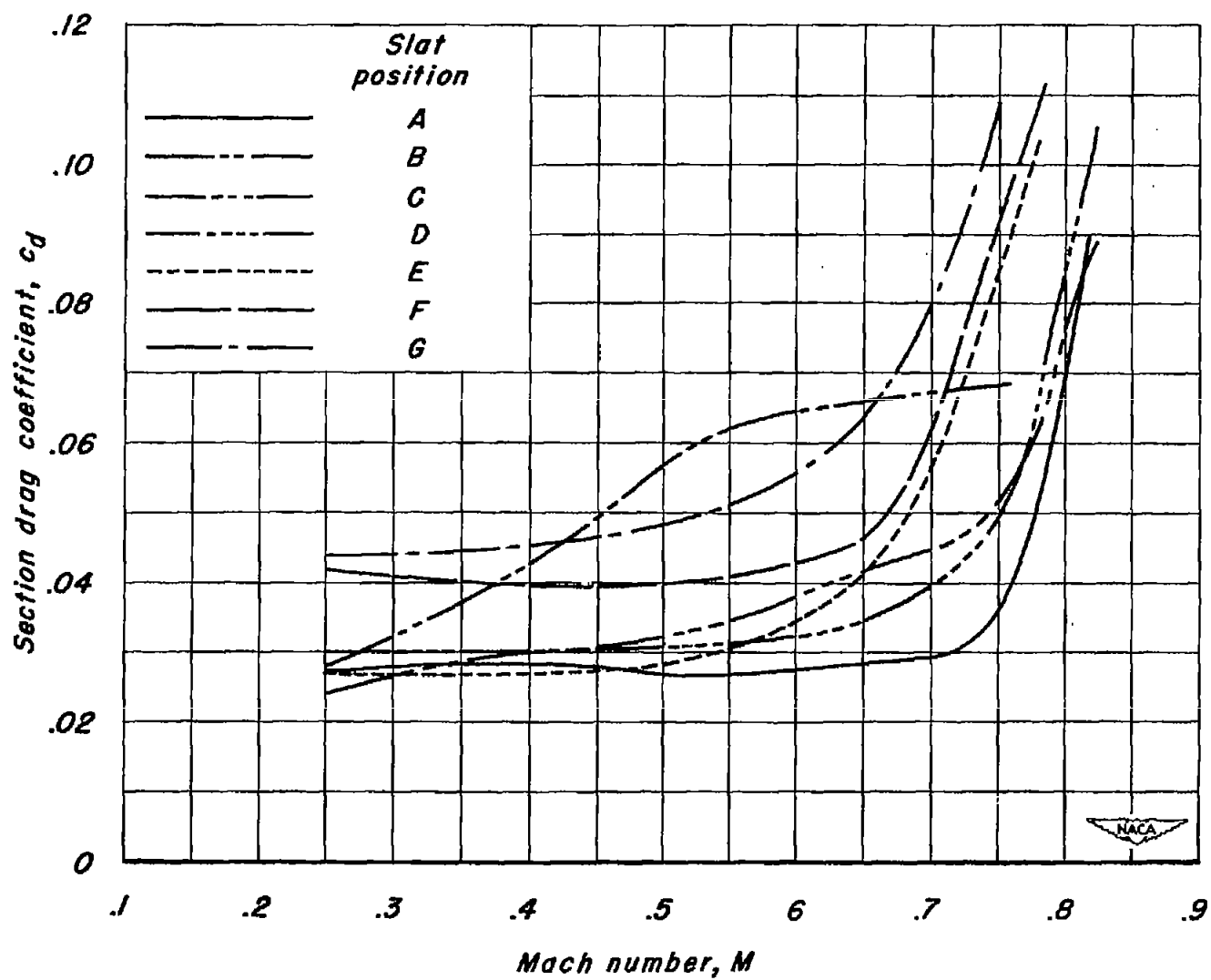


Figure 8.- Continued.



Mach number, M
 (c) c_l , 0.6
 Figure 8.- Continued.

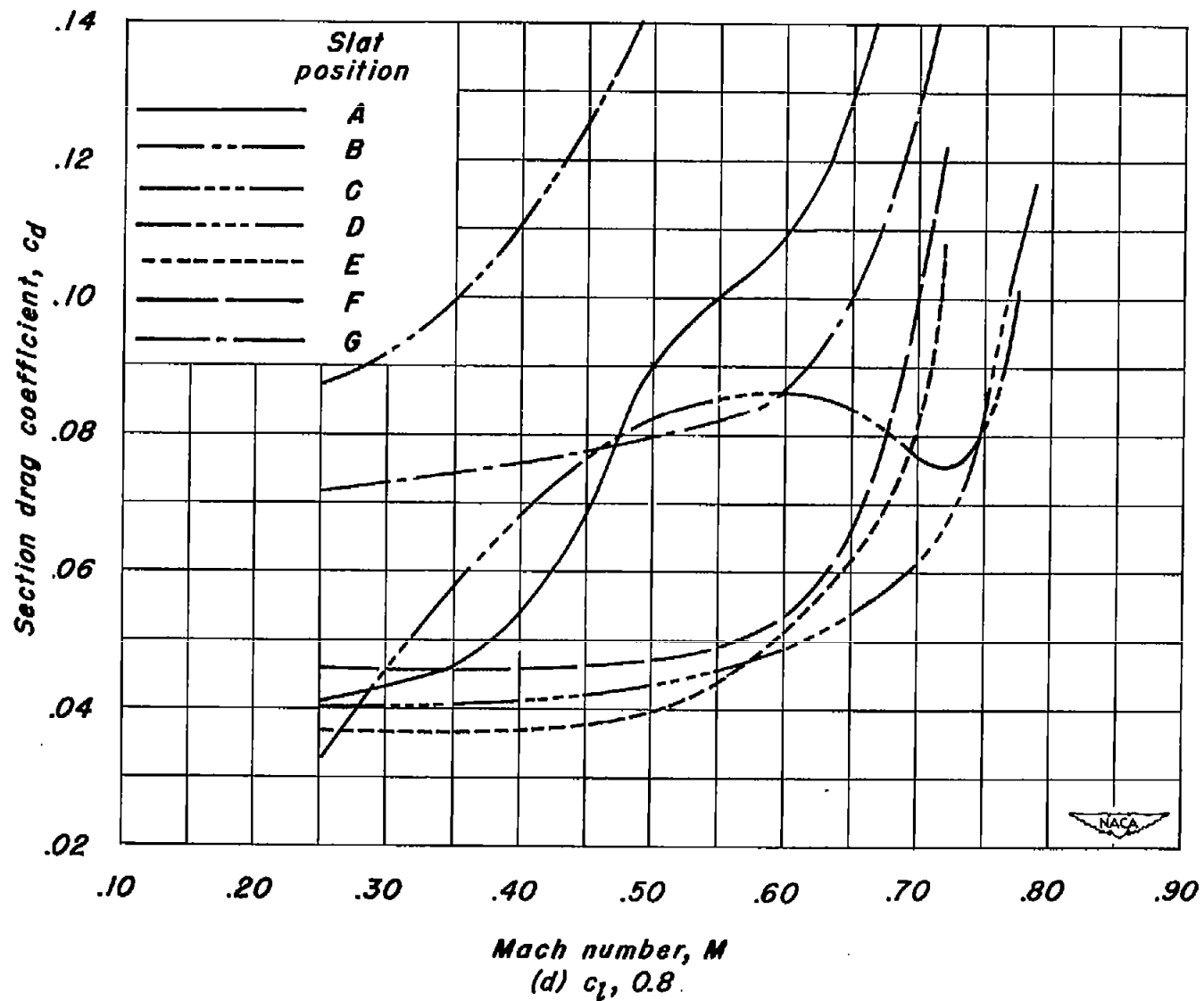
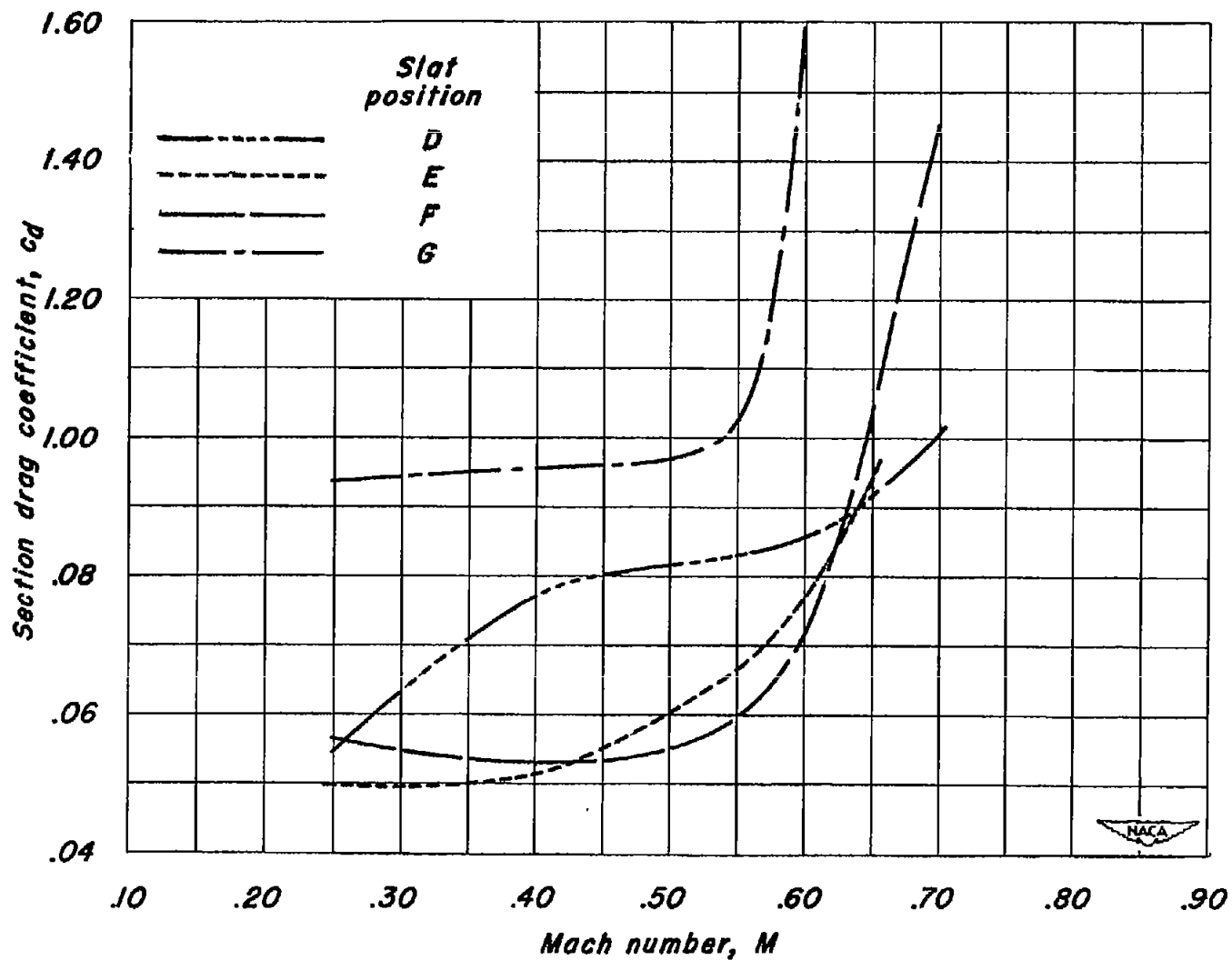


Figure 8.- Continued.



(e) c_l , 1.0.
Figure 8.- Concluded.

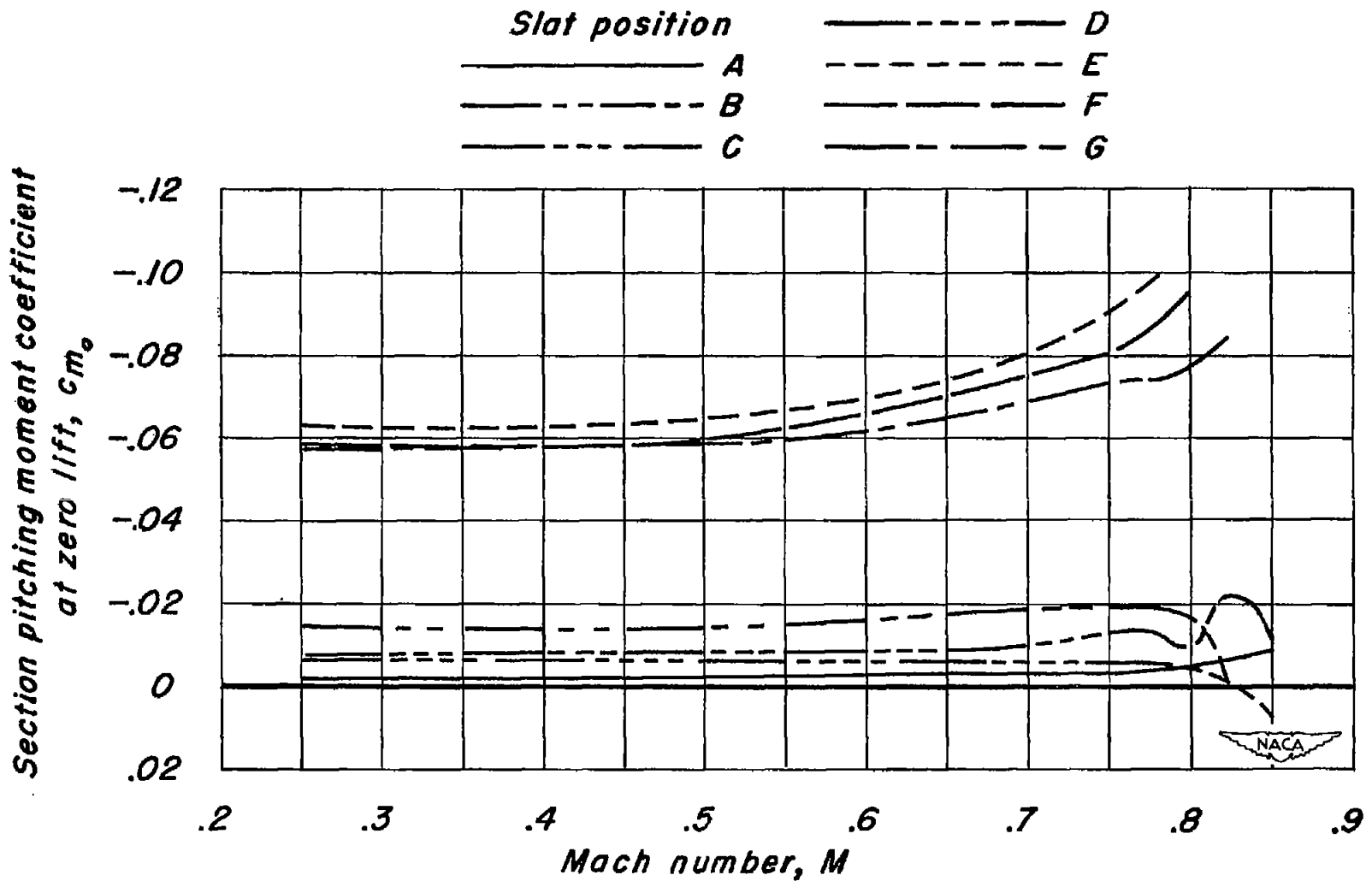


Figure 9.- Variation with Mach number of the section pitching-moment coefficient at zero lift.

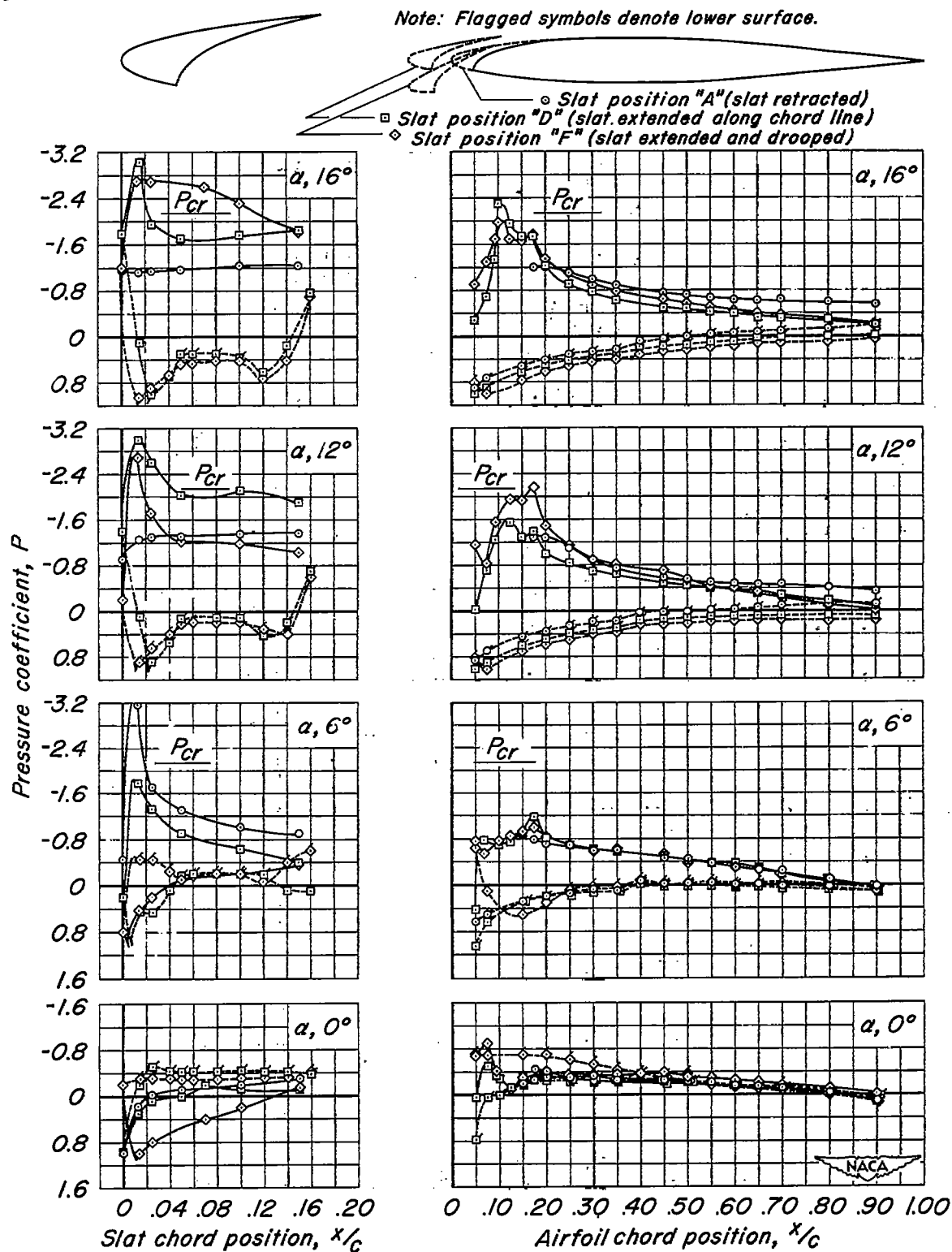
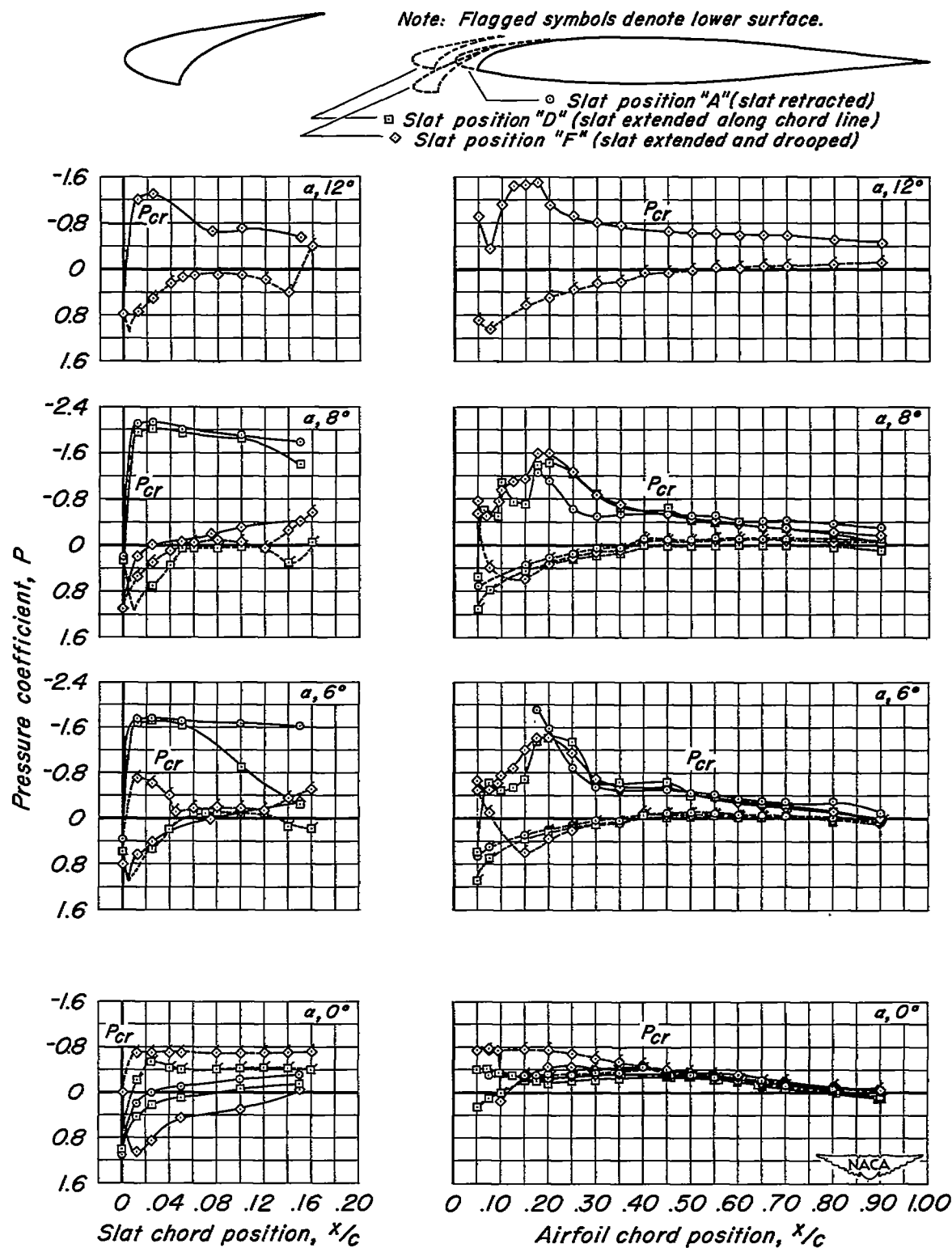
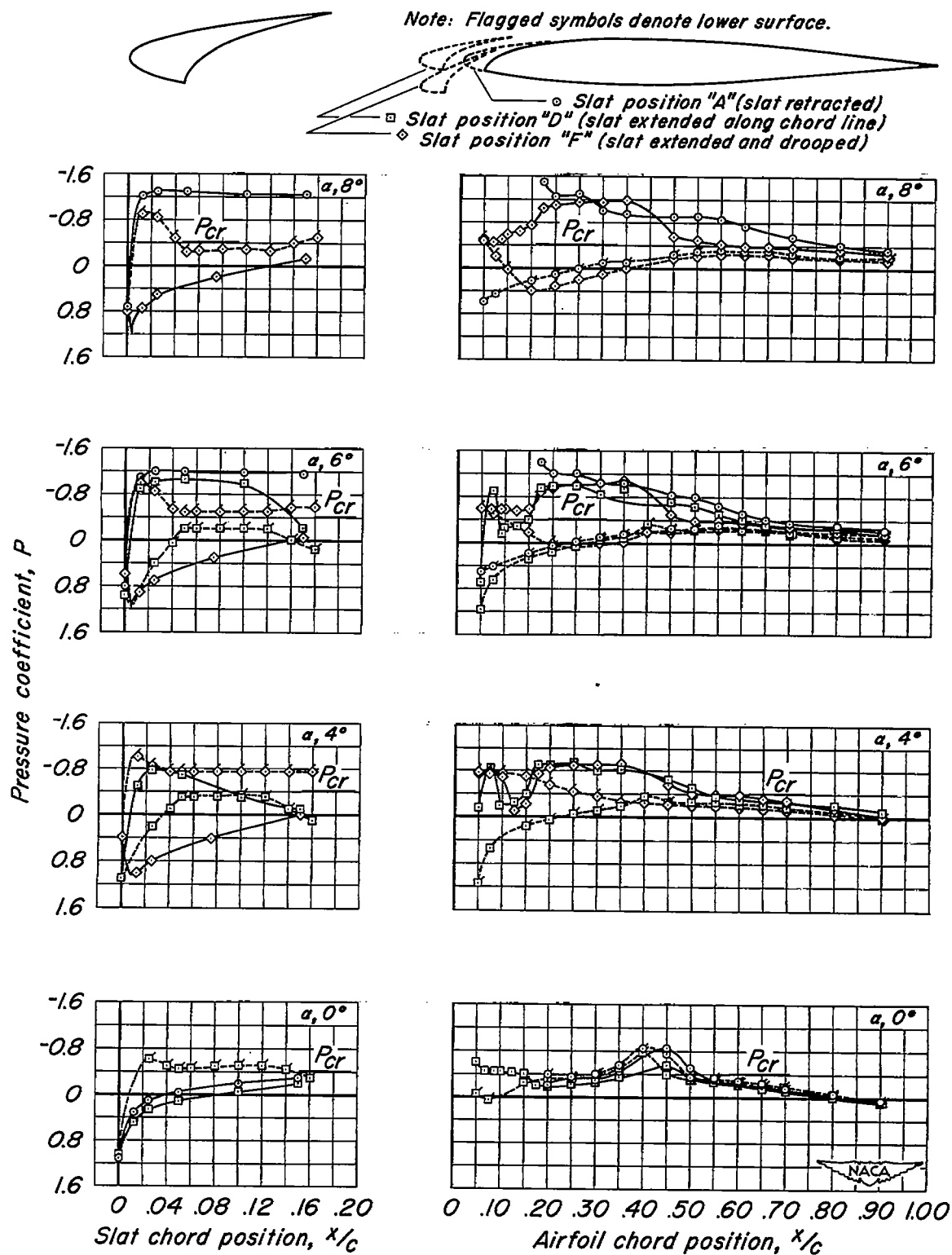
(a) $M, 0.50$

Figure 10.- Pressure distributions over the slat and airfoil at several angles of attack.



(b) $M, 0.70$.
Figure 10- Continued.



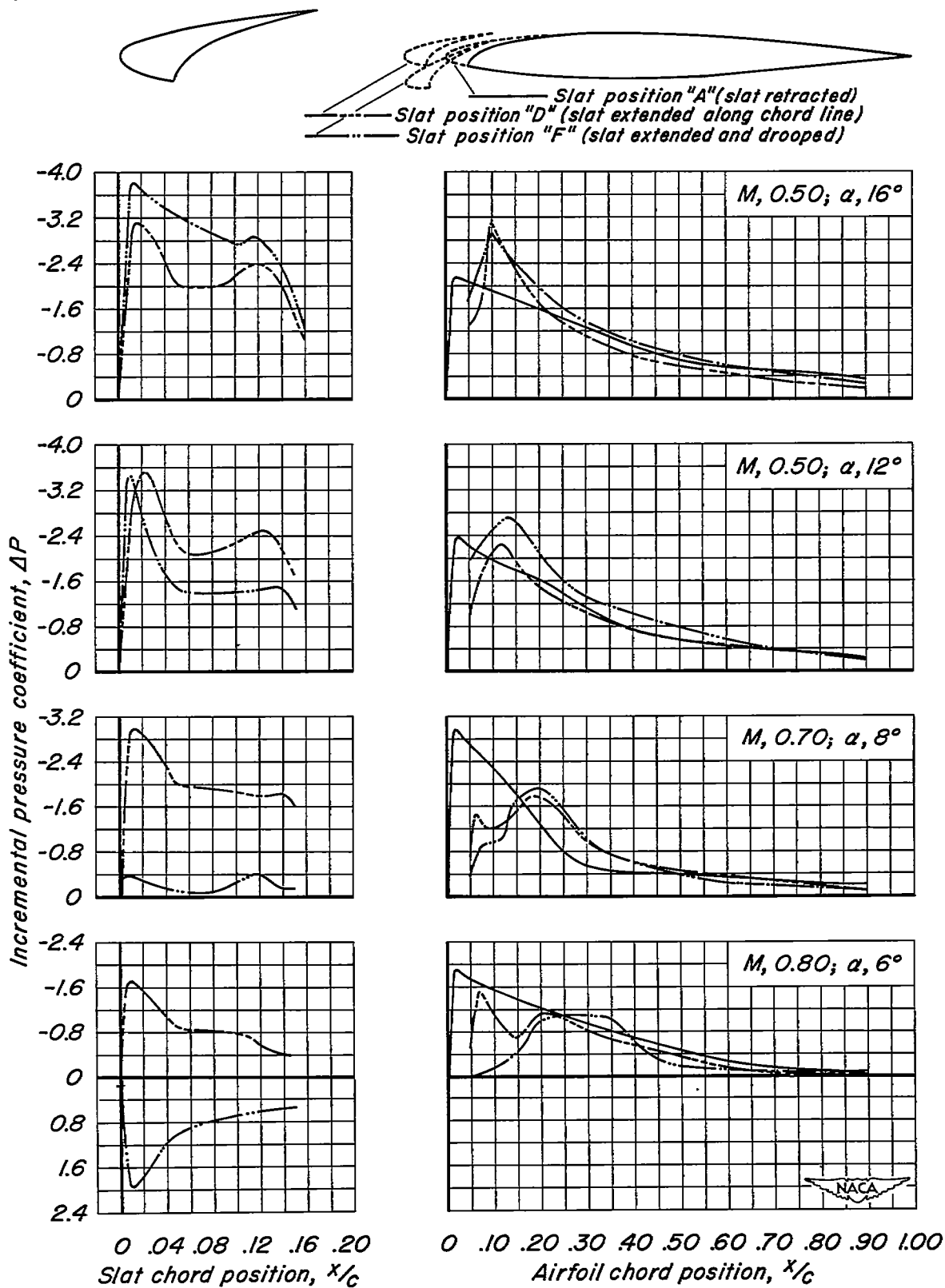


Figure 11.- Chordwise load distributions for airfoil-slat combinations A, D, and F.